# Numerical Methods for Pricing Multi-Asset Options

by

Yuwei Chen

A thesis submitted in conformity with the requirements
for the degree of Master of Science
Graduate Department of Computer Science
University of Toronto

# Abstract

Numerical Methods for Pricing Multi-Asset Options

Yuwei Chen
Master of Science
Graduate Department of Computer Science
University of Toronto
2017

We consider the pricing of two-asset European and American options by numerical Partial Differential Equation (PDE) methods, and compare the results with certain analytical formulae. Two cases of options are tested: exchange option and spread option. For exchange options, the analytical formula considered is the (exact) Margrabe formula. For spread options, we consider Kirk's formula and the formula by Li, Deng and Zhou. In pricing European two-asset options, the basic numerical PDE model is the two-dimensional Black-Scholes PDE. Different boundary conditions are considered, and the effect of them on the solution at various points of the grid is studied. Furthermore, various types of non-uniform grids are considered, aiming at reducing the error at certain areas of the grid. Moreover, the effect of the truncated domain on the PDE approximation is studied. We also discuss the effect of certain problem parameters, such as the length of maturity time, and the values of volatility and correlation, to the accuracy and convergence of the PDE approximations. The experiments indicate that the numerical PDE computed price and Greeks are second-order, for appropriately chosen grid discretizations. In the American pricing problem, the discrete penalty method is applied to the linear complementarity problem involving the two-dimensional Black-Scholes PDE and additional constraints. The convergence of the American Spread put option approximation computed with penalty iteration remains second-order, with the number of penalty iterations per timestep remaining small (2-3). We also consider an iterative method with preconditioning techniques for solving the arising large sparse linear system at each timestep, and show that this solution technique is asymptotically optimal.

# Acknowledgements

I am deelpy thankful to my supervisor, Professor Christina Christara, for her support, encouragement and guidance during my MSc program. I also thank Professor Ken Jackson for reviewing my work as a second reader, and for the valuable suggestions.

Lastly, I would like to thank all my families, and friends in my life.

# Contents

# List of Tables

# List of Figures

# Chapter 1

# Introduction

A financial derivative is a contract whose value depends on one or several underlying assets, such as stocks, currency or commodities. Options are some of the most common derivatives. A call (put) option gives the contract holder the right, but not the obligation, to buy (sell) the underlying assets at a set price on or before a certain time. When the contract holder uses this right, we say he/she exercises the option. The pre-agreed price is usually called *strike price* and the specified time is called *maturity time*. According to the exercise time, options can be classified into American and European options. American options can be exercised any time on or before maturity time while European options can only be exercised on the maturity time. Since the option holder has a right, there is a chance to earn pay-off. Therefore the option itself has a price and can be traded in option market (e.g. Chicago Board Options Exchange). Options have many practical applications, such as hedging or speculating the future asset price, hence the accurate calculation of option price is very important for an efficient and mature financial market.

In 1973, the Black-Scholes model is introduced to the option pricing problem in [2]. The Black-Scholes model is a parabolic partial differential equation (PDE) that the price of the option satisfies under certain assumptions. One important assumption is that the market is an efficient market, that is, it incorporates all relevant information. Therefore, products trade at their fair value, making it impossible for investors to find any arbitrage opportunity. Another assumption is that the underlying asset follows the geometric Brownian motion. In 1976, Merton [15] extended the Black-Scholes model to allow for jumps in the underlying assets. Other assumptions include constant volatility of asset price and constant risk-free interest rate. Although the assumptions involved in the Black-Scholes-Merton model are not necessarily realistic, practice has shown that the prices computed by the Black-Scholes-Merton model are close to the prices observed in the financial market. The Black-Scholes framework also gives a new viewpoint of risk

hedging, namely the Greeks, i.e. the derivatives of the option price. Merton and Scholes received the 1997 Nobel Prize in Economic Science for this work.

A lot of extensions to the Black-Scholes option pricing framework were proposed. One was the development of the Black-Scholes model for more complicated option contracts like the Exotic options. Another was the extension of the model itself. For example, the Heston model allows a stochastic volatility for the underlying assets.

In recent years, we often see not only univariate Call and Put options traded in the option market, but a lot of multi-asset options as well. The multi-asset options have several applications including hedging the uncertainty in the future price spreads. When pricing two-asset options such as Spread options, the Black-Scholes analysis leads to a multi-dimensional Black-Scholes PDE, which in most cases does not have a closed-form solution. Hence, such options must be priced by approximation techniques. In this thesis, numerical PDE discretization methods are used to approximate the option price. The advantage of numerical approximation is that the computed solution converges when refining the discretization size.

Besides the numerical PDE approaches, Monte Carlo (MC) simulation and lattice methods are other popular approximation methods in option pricing problems. The lattice method [10] usually simulates the stock prices paths with binomial or trinomial trees. This model traces the stock price movement in discrete-time. The MC approach [1, 7] usually simulates the stock prices paths via a discretization scheme of the stochastic differential equation (SDE) that the stock price satisfies and use these simulations to approximate the expectations of pay-offs under the risk neutral measure. These methods are easy to understand and implement. However, compared to the PDE approach, they have several shortcomings. The PDE approach is usually more accurate and efficient in low dimension problems. The numerical PDE solution is usually computed on the entire domain of the problem, while the MC and lattice methods often compute an approximate price at only one point. From this point of view, accurate hedging parameters, such as Delta and Gamma, are much easier to compute using a PDE approach rather than other methods. Another advantage of the numerical PDE approach is that it can be easily extended to some other pricing problems, which have more complicated structures, such as Asian option or Foreign exchange derivative. However, the PDE approach is usually limited in terms of the number of underlying variables, as the computational cost increases quickly with the dimension of the problem.

For the numerical solution to PDE models in finance, the most common and traditional discretization scheme is the finite difference method (FDM) in the space dimensions and Crank-Nicolson (CN) scheme in the time dimension. The CN scheme results in a

sparse linear system that need to be solved at each timestep. FDM are widely applied to option pricing problems since 1977 [19]. For problem with smooth enough solutions, the CN scheme together with the FDM has been proved to be stable and convergent. However, it has been noted that the CN scheme applied to pricing problems may exhibit undesirable oscillation behavior, because of the non-smoothness of initial condition, which is quite common for financial applications. Because of the fact, some smoothing techniques such as Rannacher smoothing timestepping [16], are applied. On the other hand, the choice of boundary conditions, such as Dirichlet boundary conditions, Neumann boundary conditions or PDE boundary conditions is critical in obtaining accurate solutions. Furthermore, in option pricing problem, the spatial domain of the underlying assets is truncated, as it is usually semi-infinite.

For American options, the Black-Scholes model results in a free boundary problem, because of the early exercise right. The free-boundary problem can be formulated as a time-dependent linear complementarity problem (LCP) with the inequalities involving the Black-Scholes PDE and some other constraints, such as that the option price must be greater than pay-off. In order to deal with the LCP in American option problem, the discrete penalty method of [6] is considered. In this approach, a penalty term is added to the PDE enforce the constraints. At each timestep, the penalty method results in a discrete non-linear equation which is solved by a penalty iteration technique. The penalty method can be extended to multiple dimensions.

Another consideration in this thesis is the efficient solution of the banded sparse linear system arising at each timestep. Because of 'the curse of dimensionality', the linear system size increases fast with the discretization size. In this case, the standard linear system solver, such as LU factorization with Gauss Elimination, may not be a smart choice. In order to take advantage of the sparsity of the arising matrices, an iterative method with a preconditioner is considered.

The thesis is organized as follows. Chapter 2 presents an introduction to financial derivatives and Black-Scholes analysis and dynamics of the underlying factors. Chapter 3 extends the Black-Scholes PDE to two dimensions and gives examples of two dimension options. Chapter 4 develops the numerical methods and techniques considered to solve the PDE-based models for the option pricing problems. In the same chapter, an iterative method with preconditioner to solve a large sparse linear system is discussed. Chapter 5 shows the numerical results of our numerical methods with several examples of multi-asset options, especially Exchange and Spread options. Chapter 6 concludes the thesis.

# Chapter 2

# Background

The Black-Scholes framework [2] explains the relationship between the prices of the options and the underlying assets in the case that the underlying assets prices follow certain stochastic processes. The Black-Scholes model makes the following assumptions:

(a) There does not exist any arbitrage opportunity in the financial market. The traders can't make instantaneous profit without any risk.

(b) The underlying asset value follows a geometric Brownian Motion

$$dS = \mu S dt + \sigma S dW \tag{2.1}$$

where $\mu$ denotes the average rate of growth of the underlying assets, $\sigma$ denotes the volatility of the asset price and $W$ is a Brownian Motion.

(c) The market is frictionless. This means there are no transaction fees, the interest rates for borrowing and lending money from and to the bank are the same, every party in market has immediate information and all entities are available at any time and in any size.

(d) No dividend will paid on the underlying asset $S$.

Under all these assumptions, it can be proved that the option price satisfies the Black-Scholes PDE. We can see that some of the assumptions are quite restrictive. For example, in the real world market, it is known that the stock price may fail to behave as a geometric Brownian motion. Merton has extended this model to allow for price jumps, which leads to a more complicated model called jump-diffusion model. However, in this chapter, we only focus on the original Black-Scholes model.

## 2.1 Black-Scholes Equation

The original Black-Scholes model is used to price the vanilla European option, which is the simplest type of option.
Black and Scholes showed that the price $u(t, S)$ of a European option driven by one underlying asset satisfies the PDE,

$$\frac{\partial u(t,S)}{\partial t} + \frac{1}{2}\sigma^2 S^2 \frac{\partial^2 u(t,S)}{\partial S^2} + rS\frac{\partial u(t,S)}{\partial S} - ru(t,S) = 0 \tag{2.2}$$

where $S$ is the asset price variable, $t$ the time variable, $\sigma$ the volatility of $S$ and $r$ the risk-free interest rate. Here we assume that $r$ and $\sigma$ are constants although they can be a function of $t$ in some more complicated models.

### 2.1.1 Derivation of Black-Scholes Equation

In the derivation of Black-Scholes Equation, we take advantage of the properties of the geometric Brownian motion and Ito's lemma. Therefore, we firstly introduce these two important tools. More details about Brownian motion, stochastic calculus and risk-neutral valuation can be found in [20] and [11].

**Definition. (Brownian motion or Wiener process)**
A Brownian motion $W(t)$ is a continuous-time stochastic process with the following properties

(a) $W(0) = 0$.

(b) $W(t) \sim \mathcal{N}(0, t)$ for all $t \geq 0$ where $\mathcal{N}(\mu, \sigma^2)$ denotes the normal distribution with expected value $\mu$ and variance $\sigma^2$. This can prove that $\mathbf{E}(dW) = 0$ and $Var(dW) = \mathbf{E}(dW^2) = dt$.

(c) The increments for non-overlapping time intervals are independent.

(d) $W(t)$ depends continuously on $t$.

**Lemma 1** ***(Itô's Lemma)***
*Let $X(t)$ be random variable which satisfies an Itô stochastic differential equation*

$$dX = a(X,t)dt + b(X,t)dW$$

*where $W$ is a Brownian motion, $a(X,t)$ is the drift coefficient and $b(X,t)$ is the diffusion coefficient. Let $g(X,t)$ be a smooth enough function of $X$. Then*

$$dg = b\frac{\partial g}{\partial X}dW + (a\frac{\partial g}{\partial X} + \frac{1}{2}b^2\frac{\partial^2 g}{\partial X^2} + \frac{\partial g}{\partial t})dt. \tag{2.3}$$

**Theorem 2** ***(Black-Scholes Equation)***
*Assume that the asset price $S$ follows a geometric Brownian motion as in (2.1). Under the assumptions of Black-Scholes framework, the call or put option price $u(t,S)$ satisfies the parabolic partial differential equation*

$$\frac{\partial u(t,S)}{\partial t} + \frac{1}{2}\sigma^2 S^2\frac{\partial^2 u(t,S)}{\partial S^2} + rS\frac{\partial u(t,S)}{\partial S} - ru(t,S) = 0. \tag{2.4}$$

**Proof**. Suppose we have a put or call option whose value is $u(t,S)$.
Now let's consider a risk-free self-financing [1] portfolio consisting of one option and $-\Delta$ shares of the underlying assets. The value of this portfolio is

$$\Pi = u - \Delta S. \tag{2.5}$$

If we assume $\Pi$ is a self-financing portfolio [2], the jump in the value of this portfolio in one time-step is

$$d\Pi = du - \Delta dS. \tag{2.6}$$

Applying Itô's lemma on option value $u(t,S)$, we can write

$$du = \sigma S\frac{\partial u}{\partial S}dW + (\mu S\frac{\partial u}{\partial S} + \frac{1}{2}\sigma^2 S^2\frac{\partial^2 u}{\partial S^2} + \frac{\partial u}{\partial t})dt. \tag{2.7}$$

Substituting (2.7) and (2.1) into (2.6) gives

$$d\Pi = \sigma S(\frac{\partial u}{\partial S} - \Delta)dW + (\mu S\frac{\partial u}{\partial S} + \frac{1}{2}\sigma^2 S^2\frac{\partial^2 u}{\partial S^2} + \frac{\partial u}{\partial t} - \mu\Delta S)dt. \tag{2.8}$$

This portfolio is kept risk-free. In order to eliminate the random component, we choose

$$\Delta = \frac{\partial u}{\partial S}. \tag{2.9}$$

[1] Self-financing means the portfolio has no exogenous infusion or withdrawal of money. Any purchase of a new asset must be financed by selling another one.

[2] The assumption of self-financing results in a property that $\Delta$ can be seen as fixed during each time increment, although, in practice, it is not. A more rigorous proof can be found in [20].

Since this portfolio is a risk-free investment, the gain in each time-step should be equal to the gain from interest in a bank, which means

$$d\Pi = (\frac{1}{2}\sigma^2 S^2 \frac{\partial^2 u}{\partial S^2} + \frac{\partial u}{\partial t})dt \equiv r\Pi dt. \tag{2.10}$$

With $\Pi = u - \frac{\partial u}{\partial S}S$, we have

$$\frac{1}{2}\sigma^2 S^2 \frac{\partial^2 u}{\partial S^2} + \frac{\partial u}{\partial t} = r(u - \frac{\partial u}{\partial S}S).$$

Rearrange the equation to get

$$\frac{\partial u(t,S)}{\partial t} + \frac{1}{2}\sigma^2 S^2 \frac{\partial^2 u(t,S)}{\partial S^2} + rS\frac{\partial u(t,S)}{\partial S} - ru(t,S) = 0. \tag{2.11}$$

□

This is the Black-Scholes equation and is a parabolic PDE. Final conditions at $t = T$ and boundary conditions are needed to ensure a unique solution to a particular type of option. For the vanilla European and the American options, the final conditions are the pay-off functions of the options.

### 2.1.2 Put Option

Put option is a kind of option which gives the holder the right to sell the underlying assets at a certain price $K$. Put option can be considered as an insurance of one's property. In the case that the price of one's asset decreases to a low level, the holder of put options can still sell the asset at price $K$.

We denote by $P(t,S)$ the price of European put option, with strike price $K$ and maturity time $T$. The **pay-off** of this put option is $(K-S)^+ = \max(K-S, 0)$.
The final condition gives the option price at $t = T$. Since, at maturity time, there will be no randomness, the option price should be equal to the pay-off function

$$P(T,S) = \max(K-S, 0). \tag{2.12}$$

This is the **final condition** for Black-Scholes Equation in the case of put options.

In the geometric Brownian motion (2.1), if $S = 0$, then $dS = 0$ and the asset price $S = 0$ will hold forever. Therefore the **boundary condition** at $S = 0$ is the time

discounted value of the final pay-off, thus

$$P(t,0) = Ke^{-r(T-t)}. \tag{2.13}$$

As $S \to \infty$, it is more and more unlikely to exercise the put option and thus

$$P(t,S) \to 0 \text{ as } S \to \infty \tag{2.14}$$

### 2.1.3 Call Option

Call option is a kind of option which gives the holder the right to buy the underlying assets at a certain price $K$. Call option can be considered as a deposit for a future investment. In the case the asset price increases to a high level, the holder of the call option can still buy the assets at price $K$.

We denote by $C(t,S)$ the price of a European call option, with strike price $K$ and maturity time $T$. The **pay-off** of this call option is $(S-K)^+ = \max(S-K,0)$.
The final condition gives the option price at maturity is given by the pay-off. Therefore the **final condition** for Black-Scholes Equation in the case of call options is

$$C(T,S) = \max(S-K,0). \tag{2.15}$$

For the same reason mentioned in put option section, if the asset price becomes zero, it will remain zero. Then the call option will have zero pay-off and it is worthless all the time. Therefore, the **boundary condition** at $S = 0$ is

$$C(t,0) = 0. \tag{2.16}$$

As the asset prices increases, it is more and more likely to exercise the call option. When $S \to +\infty$, the magnitude of strike price becomes less important. Thus, approximately,

$$C(t,S) \to S \text{ as } S \to +\infty. \tag{2.17}$$

However, if we consider the time-discounted strike price, a more accurate boundary condition for the far side is

$$C(t,S) \approx S - Ke^{-r(T-t)}. \tag{2.18}$$

### 2.1.4 Analytical Solution

Here we quote the analytical formula of the solution to the Black-Scholes PDE with call and put final conditions. The formulae [10] for European call and put options are,

$$C = S\Phi(d_1) - Ke^{-r(T-t)}\Phi(d_2) \tag{2.19}$$

and

$$P = Ke^{-r(T-t)}\Phi(-d_2) - S\Phi(-d_1) \tag{2.20}$$

where

$$d_1 = \frac{\log(S/K) + (r + \sigma^2/2)(T-t)}{\sigma\sqrt{T-t}}$$
$$d_2 = \frac{\log(S/K) + (r - \sigma^2/2)(T-t)}{\sigma\sqrt{T-t}} = d_1 - \sigma\sqrt{T-t}$$

where $\Phi$ is the cumulative density function (CDF) of the standard normal distribution.

## 2.2 American Options

Compared to European options, American options allow the contract holder to exercise the option any time on or before the maturity time. Since the American option gives the holder more right than the European option, it is expected to have a higher price. We also note that the value of the American option at any time cannot be less than the pay-off. Otherwise the option gives the arbitrage opportunity. Therefore, the pay-off function can be seen as an obstacle for the price of American options when using the Black-Scholes framework.

We present the formulation of the American option problem as a linear complementarity problem (LCP) [21].

Let's assume $u(t, S)$ is the value of American option and the pay-off is $f(S)$. Then the American option pricing problem can be stated as

$$\left\{ \begin{array}{c} \frac{\partial u}{\partial \tau} - Lu = 0 \\ u - f \geq 0 \end{array} \right\} \vee \left\{ \begin{array}{c} \frac{\partial u}{\partial \tau} - Lu \geq 0 \\ u - f = 0 \end{array} \right\} \tag{2.21}$$

where

$$Lu \equiv -\frac{1}{2}\sigma^2 S^2 \frac{\partial^2 u(t,S)}{\partial S^2} - rs\frac{\partial u(t,S)}{\partial S} + ru(t,S) \tag{2.22}$$

and the notation $\vee$ means "or". Typically at each time $t$, there is a particular asset price which divides the asset price domain into two regions: the side suggesting holding options corresponding to the left conditions in (2.21) and the side suggesting early exercise corresponding to the right conditions in (2.21). This particular value of $S$ is unknown and is usually called *free boundary*.

For the American put option, the final conditions are the $f(S)$ is the pay-off at maturity and the boundary conditions are

$$u(t,0) = K \tag{2.23}$$

$$u(t,S) \to 0 \text{ as } S \to \infty. \tag{2.24}$$

## 2.3 Greeks

In finance, Greeks are the sensitivities of the financial derivatives price to the movement of various parameters or variables, and are also called *risk sensitivities* or *hedging parameters*. These parameters are essential tools in risk management. For example, in the derivation of the Black-Scholes equation, we use an idea of Delta-hedging. This is a dynamic strategy to keep a portfolio risk-free by re-balancing the portfolio, more specifically, the ratio of options and underlying assets. Although in practice, this technique needs adjustment to take into account the transaction costs, the general idea of keeping a portfolio risk-free is based on the accurate calculation of the Greeks.
In Delta-hedging, **Delta** is the rate of change of the price of the option with respect to the change of the price of underlying assets. Mathematically, it can be written as

$$\Delta = \frac{\partial u}{\partial S}. \tag{2.25}$$

In some other hedging strategy, we may only need to hedge away the risk due to the changes of underlying asset's Delta. The **Gamma** is given by

$$\Gamma = \frac{\partial^2 u}{\partial S^2}. \tag{2.26}$$

The time decay of the value for a derivative is called **theta**, given by

$$\Theta = \frac{\partial u}{\partial t}. \tag{2.27}$$

**Vega** measures the sensitivity to the volatility, given by

$$\nu = \frac{\partial u}{\partial \sigma}. \tag{2.28}$$

# Chapter 3

# Multi-Asset Black-Scholes Equation

In the option market, a lot of traded options are multi-asset options. Multi-asset options are a group of options whose pay-off depends on more than one underlying assets. In this sense, a two-asset option is a special case of multi-asset option, where the number of underlying assets is two. In this case, we say this option is two-dimensional. If we extend the Black-Scholes framework to two-asset options, the corresponding Black-Scholes equation becomes a two-dimensional parabolic PDE with the two asset prices playing the role of the respective space variables.

A typical example of multi-asset options is the basket option. This option is based on two or more underlying stocks. In European Basket call option, the overall value of a basket of assets plays the role of the price of the underlying asset in single-asset European call option. If the weighted summation of all the stock prices in the basket is above the strike price, option-holders are encouraged to exercise the option and buy all the stocks in the basket. Multi-asset options can still have European and American type, as far as the time of exercising is concerned.

In our work, we primarily focus on numerically pricing two-asset spread options, whose pay-off focuses on the difference of the prices of the two underlying assets. However, our model and numerical methods are applicable to various types of two-dimensional option contracts. In this chapter, we will show the two-dimensional Black-Scholes model and several common examples of two-asset options.

## 3.1 Two-Dimensional Black-Scholes Equation

Consider a European option whose pay-off $f(S_1, S_2)$ depends on the prices of two underlying assets $S_1$ and $S_2$. With the same assumptions of the Black-Scholes framework,

suppose each asset price follows a geometric Brownian motion

$$dS_1 = S_1(\mu_1 dt + \sigma_1 dW_1), \tag{3.1}$$

$$dS_2 = S_2(\mu_2 dt + \sigma_2 dW_2). \tag{3.2}$$

Each $dW_i$, for $i = 1, 2$, satisfies

$$\mathbf{E}(dW_i) = 0 \text{ and } \mathbf{E}(dW_i^2) = dt. \tag{3.3}$$

At the same time, we assume these the two underlying assets are correlated:

$$corr(W_1, W_2) = \rho \text{ or } \mathbf{E}(dW_1 dW_2) = \rho dt. \tag{3.4}$$

Here we say that $\rho$ is the correlation between the two stochastic process $W_1$ and $W_2$.

**Theorem 3** ***(Two-Dimensional Black-Scholes Equation)***
*Suppose the two underlying assets follow the correlated geometric Brownian motions (3.1) and (3.2) with correlation as in (3.4). Under the assumptions of the Black-Scholes framework, the two-asset option price $u(t, S_1, S_2)$ satisfies the partial differential equation*

$$\frac{\partial u}{\partial t} + \frac{1}{2}\sigma_1^2 S_1^2 \frac{\partial^2 u}{\partial S_1^2} + \frac{1}{2}\sigma_2^2 S_2^2 \frac{\partial^2 u}{\partial S_2^2} + \rho\sigma_1\sigma_2 S_1 S_2 \frac{\partial^2 u}{\partial S_1 \partial S_2} + rS_1 \frac{\partial u}{\partial S_1} + rS_2 \frac{\partial u}{\partial S_2} - ru = 0. \tag{3.5}$$

**Proof**. The basic idea is same as the original Black-Scholes Equation. Suppose the option price is $u(t, S_1, S_2)$.
We assume there is a risk-free self-financing portfolio

$$\Pi = u - \Delta_1 S_1 - \Delta_2 S_2. \tag{3.6}$$

consisting of one share of option, $-\Delta_1$ shares of first underlying asset and $-\Delta_2$ shares of second underlying asset. Then the increment [1] is

$$d\Pi = du - \Delta_1 dS_1 - \Delta_2 dS_2. \tag{3.7}$$

[1] This is a result of self-financing assumption. With self-financing assumption, $\Delta_1$ and $\Delta_2$ can be seen as constant during each time increment, although, in practice, they are not. A more rigorous treatment of this self-financing property can be found in [20].

Applying Itô's lemma on the two-dimensional function $u(t, S_1, S_2)$, we can write

$$\begin{aligned} du =&\sigma_1 S_1 \frac{\partial u}{\partial S_1} dW_1 + \sigma_2 S_2 \frac{\partial u}{\partial S_2} dW_2 + (\frac{\partial u}{\partial t} + \mu_1 S_1 \frac{\partial u}{\partial S_1} + \mu_2 S_2 \frac{\partial u}{\partial S_2} \\ &+ \frac{1}{2}\sigma_1^2 S_1^2 \frac{\partial^2 u}{\partial S_1^2} + \rho\sigma_1\sigma_2 S_1 S_2 \frac{\partial^2 u}{\partial S_1 \partial S_2} + \frac{1}{2}\sigma_2^2 S_2^2 \frac{\partial^2 u}{\partial S_2^2})dt. \end{aligned} \tag{3.8}$$

Substituting (3.8), (3.1) and (3.2) into (3.7) gives,

$$\begin{aligned} d\Pi =&\sigma_1 S_1 (\frac{\partial u}{\partial S_1} - \Delta_1) dW_1 + \sigma_2 S_2 (\frac{\partial u}{\partial S_2} - \Delta_2) dW_2 + (\frac{\partial u}{\partial t} + \mu_1 S_1 \frac{\partial u}{\partial S_1} + \mu_2 S_2 \frac{\partial u}{\partial S_2} \\ &+ \frac{1}{2}\sigma_1^2 S_1^2 \frac{\partial^2 u}{\partial S_1^2} + \rho\sigma_1\sigma_2 S_1 S_2 \frac{\partial^2 u}{\partial S_1 \partial S_2} + \frac{1}{2}\sigma_2^2 S_2^2 \frac{\partial^2 u}{\partial S_2^2} - \mu_1 \Delta_1 S_1 - \mu_2 \Delta_2 S_2)dt. \end{aligned} \tag{3.9}$$

In order to eliminate the randomness of portfolio $\Pi$, we set

$$\Delta_1 = \frac{\partial u}{\partial S_1}, \Delta_2 = \frac{\partial u}{\partial S_2}. \tag{3.10}$$

The return of this portfolio should be equal to the return from risk-free interest rate, which means

$$d\Pi = (\frac{\partial u}{\partial t} + \frac{1}{2}\sigma_1^2 S_1^2 \frac{\partial^2 u}{\partial S_1^2} + \rho\sigma_1\sigma_2 S_1 S_2 \frac{\partial^2 u}{\partial S_1 \partial S_2} + \frac{1}{2}\sigma_2^2 S_2^2 \frac{\partial^2 u}{\partial S_2^2})dt = r\Pi dt. \tag{3.11}$$

Therefore,

$$\frac{\partial u}{\partial t} + \frac{1}{2}\sigma_1^2 S_1^2 \frac{\partial^2 u}{\partial S_1^2} + \rho\sigma_1\sigma_2 S_1 S_2 \frac{\partial^2 u}{\partial S_1 \partial S_2} + \frac{1}{2}\sigma_2^2 S_2^2 \frac{\partial^2 u}{\partial S_2^2} = r(u - \frac{\partial u}{\partial S_1} S_1 - \frac{\partial u}{\partial S_2} S_2). \tag{3.12}$$

Rearrange the terms to get the two-dimensional Black-Scholes equation,

$$\frac{\partial u}{\partial t} + \frac{1}{2}\sigma_1^2 S_1^2 \frac{\partial^2 u}{\partial S_1^2} + \rho\sigma_1\sigma_2 S_1 S_2 \frac{\partial^2 u}{\partial S_1 \partial S_2} + \frac{1}{2}\sigma_2^2 S_2^2 \frac{\partial^2 u}{\partial S_2^2} + rS_1 \frac{\partial u}{\partial S_1} + rS_2 \frac{\partial u}{\partial S_2} - ru = 0. \tag{3.13}$$

□

## 3.2 Examples of Two-Asset Options

### 3.2.1 Exchange Option

Exchange option is commonly seen in the energy market. It is a special kind of Spread option when the strike price is zero. It is also one of the simplest multi-asset options. The pay-off of Exchange is

$$\max(S_1 - S_2, 0) \tag{3.14}$$

Since there is no strike price term, the typical classification of call and put option is not appropriate for Exchange option. However, we can still consider the first asset $S_1$ being on the call position while the second asset $S_2$ being on the put position.

#### Margrabe formula

In 1978, Margrabe [14] developed an analytical solution formula to Black-Scholes Equation for Exchange option. Suppose $C(t, S_1, S_2)$ is the price of Exchange option at time $t$ with the two asset prices being $S_1$ and $S_2$. Then the formula is given

$$C(t, S_1, S_2) = S_1\Phi(d_1) - S_2\Phi(d_2).$$

where

$$\begin{aligned}
\sigma &= \sqrt{\sigma_1^2 + \sigma_2^2 - 2\rho\sigma_1\sigma_2}, \\
d_1 &= \frac{\log(S_1/S_2) + (\frac{\sigma^2}{2})(T-t)}{\sigma\sqrt{T-t}}, \\
d_2 &= \frac{\log(S_1/S_2) - (\frac{\sigma^2}{2})(T-t)}{\sigma\sqrt{T-t}} = d_1 - \sigma\sqrt{T-t}.
\end{aligned}$$

#### Boundary Conditions

The domain for each of the asset prices is a semi-infinite domain $[0, +\infty]$. In a numerical method, we usually truncate the domain to $[0, S_{1,\infty}]$ and $[0, S_{2,\infty}]$, respectively. The choice of the far-sides $S_{1,\infty}$ and $S_{2,\infty}$ usually depends on which evaluation area we are interested in. The numerical parameters $S_{1,\infty}$ and $S_{2,\infty}$ are set sufficiently large compared to the evaluation area coordinates. In general, larger $S_{1,\infty}$ and $S_{2,\infty}$ give better accuracy.

The zero-side boundary conditions are

$$u(t, 0, S_2) = 0 \tag{3.15}$$

$$u(t, S_1, 0) = S_1. \tag{3.16}$$

We considered three different types of boundary condition on the far-side boundaries.

- Margrabe Boundary Conditions
  For Exchange option, the analytical solution is available. In this case, it is natural to use the analytical formula to generate the boundary conditions. Suppose $C(t, S_1, S_2)$ is given in 3.15, then the far-side boundary conditions are

$$u(t, S_{1,\infty}, S_2) = C(t, S_{1,\infty}, S_2) \tag{3.17}$$

$$u(t, S_1, S_{2,\infty}) = C(t, S_1, S_{2,\infty}). \tag{3.18}$$

- Pay-off Boundary Conditions
  Pay-off functions are reasonably accurate approximations to far-side boundary conditions as well. They are given by

$$u(t, S_{1,\infty}, S_2) = \max(S_{1,\infty} - S_2, 0) \tag{3.19}$$

$$u(t, S_1, S_{2,\infty}) = \max(S_1 - S_{2,\infty}, 0) \tag{3.20}$$

  However, the pay-off boundary conditions are not so accurate when $S_1$ and $S_2$ are both reaching the far-side boundary.

- PDE Boundary Conditions
  It is natural to assume that the points on the far-side boundary satisfy the Black-Scholes equation. Therefore, we consider to use the PDE

$$\frac{\partial u}{\partial t} + \frac{1}{2}\sigma_1^2 S_1^2 \frac{\partial^2 u}{\partial S_1^2} + \rho\sigma_1\sigma_2 S_1 S_2 \frac{\partial^2 u}{\partial S_1 \partial S_2} + \frac{1}{2}\sigma_2^2 S_2^2 \frac{\partial^2 u}{\partial S_2^2} + rS_1 \frac{\partial u}{\partial S_1} + rS_2 \frac{\partial u}{\partial S_2} - ru = 0. \tag{3.21}$$

  as the far-side boundary condition.

We note that Margrabe boundary conditions are the natural conditions to consider for Exchange options. However, we also consider pay-off and PDE boundary conditions for testing purposes, as those are useful when there is no analytical formula for the price of options available.

### 3.2.2 Spread Option

Spread Option is a two-asset option written on the difference between the prices of two underlying entities. It is widely used in currency markets, energy markets, etc.

In the currency markets, spread options are common in the foreign exchange. The Spread option is often seen in the currency exchange between the currencies of two countries whose economies are closely related. A typical example of Spread option is cross-currency option that involves the exchange of two currencies against one base currency. In a cross-currency option, $S_1$ and $S_2$ are the exchange rates of two foreign currencies measured in some base currency.

In the energy market, the spread options are often used to hedge against the fluctuation of the price margins in the energy product refinement industry. The most frequently mentioned Spread options are the Crack and Spark Spread options. Crack Spread option allows simultaneous purchase or sale of crude oil against the sale or purchase, respectively, of the refined petroleum product,. It is an insurance in the case of the sharp move of the price of crude oil or refined petroleum products. Spark Spread option can be seen in electricity market. In this Spread option, one underlying asset is electricity price, while another underlying asset is the price of the natural gas used to generate the electricity. So this option can be seen as a proxy for the cost of converting gas into electricity.

The pay-off of spread is

$$\max(S_1 - S_2 - K, 0) \text{ for Spread call option} \tag{3.22}$$

$$\max(K - (S_1 - S_2), 0) \text{ for Spread put option} \tag{3.23}$$

where $K$ is the strike price.

#### Analytical Approximations

For Spread options, there is no analytical formulae that gives the prices. However, lots of analytical approximations have been proposed. We introduce some famous closed-form approximations in this section.

- **Kirk's formula**
  In 1995, Kirk [12] suggests a closed-form approximation to Spread call option price. It reads as follows:

$$C(t, S_1, S_2) \approx S_1\Phi(d_1) - (S_2 + Ke^{-r(T-t)})\Phi(d_2). \tag{3.24}$$

where

$$\sigma = \sqrt{\sigma_1^2 + \sigma_2^2(\frac{S_2}{S_2+K})^2 - 2\rho\sigma_1\sigma_2\frac{S_2}{S_2+K}},$$
$$d_1 = (\log(\frac{S_1}{S_2+K}) + (\frac{\sigma^2}{2})(T-t))/(\sigma\sqrt{T-t}),$$
$$d_2 = (\log(\frac{S_1}{S_2+K}) - (\frac{\sigma^2}{2})(T-t))/(\sigma\sqrt{T-t}) = d_1 - \sigma\sqrt{T-t}.$$

- **Li, Deng and Zhou's Approximation**

  In 2008, Li, Deng and Zhou [13] proposed another closed-form approximation to Spread call option price. They suggested that under the joint-normal set-up, the price of the Spread call option is given by

$$C(t, S_1, S_2) \approx e^{v_1^2/2+\hat{\mu_1}-r(T-t)}I_1 - e^{v_2^2/2+\hat{\mu_2}-r(T-t)}I_2 - Ke^{-r(T-t)}I_3. \tag{3.25}$$

  For $i = 1, 2, 3$, the integrals $I_i$ are approximated to second order in $\epsilon$ as

$$I_i \approx J_0(C_i, D_i) + J_1(C_i, D_i)\epsilon + \frac{1}{2}J_2(C_i, D_i)\epsilon^2 \tag{3.26}$$

  where the functions $J_i$'s are defined as

$$J_0(u, v) = \Phi(\frac{u}{\sqrt{1+v^2}}) \tag{3.27}$$
$$J_1(u, v) = \frac{1+(1+u^2)v^2}{(1+v^2)^{5/2}}\mathbf{N}(\frac{u}{\sqrt{1+v^2}}) \tag{3.28}$$
$$J_2(u, v) = \frac{(6-6u^2)v^2 + (21-2u^2-u^4)v^4 + 4(3+u^2)v^6 - 3}{(1+v^2)^{11/2}}u \cdot \mathbf{N}(\frac{u}{\sqrt{1+v^2}}) \tag{3.29}$$

and $C_i$, $D_i$ and $\epsilon$ are given by

$$
\begin{aligned}
C_1 &= C_3 + D_3\rho v_1 + \epsilon\rho^2 v_1^2 + \sqrt{1-\rho^2}v_1 \\
D_1 &= D_3 + 2\rho v_1\epsilon \\
C_2 &= C_3 + D_3 v_2 + \epsilon v_2^2 \\
D_2 &= D_3 + 2v_2\epsilon \\
C_3 &= \frac{1}{v_1\sqrt{1-\rho^2}}(\mu_1 - \log(R+K) + \frac{v_2 R}{R+K}\gamma_0 - \frac{1}{2}\frac{v_2^2 RK}{(R+K)^2}\gamma_0^2) \\
D_3 &= \frac{1}{v_1\sqrt{1-\rho^2}}(\rho v_1 - \frac{v_2 R}{R+K} + \frac{v_2^2 RK}{(R+K)^2}\gamma_0) \\
\epsilon &= -\frac{1}{2v_1\sqrt{1-\rho^2}}\frac{v_2^2 RK}{(R+K)^2} \\
R &= e^{v^2\gamma_0+\mu_2} \\
\mu_i &= \log S_i + (r - \sigma_i^2/2)(T-t), i = 1,2 \\
v_i &= \sigma_i\sqrt{T-t}, i = 1,2.
\end{aligned}
$$

In this formula, $\mathbf{N}(x)$ is the probability density function (PDF) of standard normal distribution and $\Phi(x)$ is the the CDF of standard normal distribution. The parameter $\gamma_0$ is any real number close to zero and generally we set $\gamma_0 = 0$.

**Boundary Conditions**

For Spread options, we consider the following boundary conditions.

- Pay-off Boundary Conditions
  Time-discounted pay-off functions are reasonably accurate approximations to boundary values of Spread options.
  The discounted pay-off boundary conditions for Spread call option are

$$
\begin{aligned}
u(t,0,S_2) &= \max(-Ke^{-r(T-t)} - S_2, 0) = 0, && (3.30)\\
u(t,S_1,0) &= \max(S_1 - Ke^{-r(T-t)}, 0), && (3.31)\\
u(t,S_{1,\infty},S_2) &= \max(S_{1,\infty} - S_2 - Ke^{-r(T-t)}, 0), && (3.32)\\
u(t,S_1,S_{2,\infty}) &= \max(S_1 - S_{2,\infty} - Ke^{-r(T-t)}, 0). && (3.33)
\end{aligned}
$$

The discounted pay-off boundary conditions for Spread put option are

$$u(t, 0, S_2) = \max(Ke^{-r(T-t)} + S_2, 0), \tag{3.34}$$
$$u(t, S_1, 0) = \max(Ke^{-r(T-t)} - S_1, 0), \tag{3.35}$$
$$u(t, S_{1,\infty}, S_2) = \max(Ke^{-r(T-t)} - (S_{1,\infty} - S_2), 0), \tag{3.36}$$
$$u(t, S_1, S_{2,\infty}) = \max(Ke^{-r(T-t)} - (S_1 - S_{2,\infty}), 0). \tag{3.37}$$

- Alternative Boundary Conditions
  As we take a deeper look at equations (3.31) and (3.35), we can find they are exactly the pay-off function for European options written on a single underlying asset. Therefore, the solution to the one-asset Black-Scholes equation can be a more accurate boundary condition for $u(t, S_1, 0)$. For Spread call option, when $S_2 = 0$, we take the value of the closed-form solution of the Black-Scholes equation of a call option for $S_1$ with strike price $K$. For Spread put option, when $S_1 = 0$, we take the value of the closed-form solution of the Black-Scholes equation of a put option for $S_2$ with strike price $K$.

### 3.2.3 Basket Option

A Basket option gives the holder the option to buy or sell a group of underlying assets at the same time. The pay-off function of Basket option depends on the weighted sum of the underlying assets and is given by

$$\max(\sum_{i=1}^{2} w_i S_i - K, 0) \text{ for Basket call option,} \tag{3.38}$$
$$\max(K - \sum_{i=1}^{2} w_i S_i, 0) \text{ for Basket put option,} \tag{3.39}$$

where $w_i$ is the weight of $i^{th}$ asset in basket option contract. Although it is not necessary, we prefer to set the summation of the weights to one, i.e. $\sum_{i=1}^{2} w_i = 1$.

#### Boundary Conditions

For Basket options, we consider the following boundary conditions.

- Pay-off Boundary Conditions
  Time-discounted Pay-off functions are reasonably accurate approximations to boundary values of Basket option.

The pay-off boundary conditions for Basket call options are

$$u(t,0,S_2) = \max(w_2S_2 - Ke^{-r(T-t)}, 0), \tag{3.40}$$
$$u(t,S_1,0) = \max(w_1S_1 - Ke^{-r(T-t)}, 0), \tag{3.41}$$
$$u(t,S_{1,\infty},S_2) = \max(w_1S_{1,\infty} + w_2S_2 - Ke^{-r(T-t)}, 0), \tag{3.42}$$
$$u(t,S_1,S_{2,\infty}) = \max(w_1S_1 + w_2S_{2,\infty} - Ke^{-r(T-t)}, 0). \tag{3.43}$$

The pay-off boundary conditions for Basket put option are

$$u(t,0,S_2) = \max(Ke^{-r(T-t)} - w_2S_2, 0), \tag{3.44}$$
$$u(t,S_1,0) = \max(Ke^{-r(T-t)} - w_1S_1, 0), \tag{3.45}$$
$$u(t,S_{1,\infty},S_2) = \max(Ke^{-r(T-t)} - (w_1S_{1,\infty} + w_2S_2), 0), \tag{3.46}$$
$$u(t,S_1,S_{2,\infty}) = \max(Ke^{-r(T-t)} - (w_1S_1 + w_2S_{2,\infty}), 0). \tag{3.47}$$

- Alternative Boundary Conditions
  As we can see, equations (3.40) and (3.41) can be seen as the pay-off functions of vanilla European call options on a single underlying asset. Therefore when $S_1 = 0$, we can use the solution to the Black-Scholes equation of call option with asset $w_2S_2$ and strike $K$ as a boundary condition. When $S_2 = 0$, we can use the solution to the Black-Scholes equation of call option with asset $w_1S_1$ and strike $K$ as a boundary condition.

  With the same idea, the equations (3.44) and (3.45) can be seen as pay-off functions of vanilla put European options on a single underlying asset. Therefore when $S_1 = 0$, we can use the solution to the Black-Scholes equation of put option with asset $w_2S_2$ and strike $K$ as a boundary condition. When $S_2 = 0$, we can use the solution to the Black-Scholes equation of put option with asset $w_1S_1$ and strike $K$ as a boundary condition.

### 3.2.4 Rainbow Option

Rainbow option is also a multi-asset option. There are various different forms of Rainbow option on the market. However, the common idea of Rainbow options is to have a pay-off that is depending on the assets sorted by their performance at maturity. These are some typical examples of Rainbow option:

| Name | Pay-off |
|---|---|
| Multi-strike Rainbow option | $\max\{S_1 - K_1, S_2 - K_2, 0\}$ |
| Pyramid Rainbow option | $\max\{\lvert S_1 - K_1\rvert + \lvert S_2 - K_2\rvert - K, 0\}$ |
| Max option | $\max\{S_1, S_2\}$ |
| Rainbow max call option | $\max\{\max\{S_1, S_2\} - K, 0\}$ |

Table 3.1: Rainbow Options

# Chapter 4

# Numerical Methods

As discussed in Chapter 3, we have shown that European or American two-asset option pricing problems result in a two-dimensional Black-Scholes PDE which is a parabolic PDE with variables the time $t$ and the two asset prices, $S_1$ and $S_2$. Different two-asset options are defined by different pay-off functions. For some simple pricing problems, such as vanilla European Exchange option, the closed-form analytical formula for the solution is easily obtained. However, in most of the two-asset options or American type options, no closed-form analytical solution is known. Therefore, numerical methods are required to compute approximate solutions.

Finite difference methods (FDMs) are numerical methods for solving differential equations. These methods are widely used in mathematical finance for the valuation of options since 1977 [19].The idea of FDMs is to discretize the domain with several grid points and use finite differences to approximate the derivatives on these grid points. After finite difference discretization along the space and time dimensions to the Black-Scholes PDE has been applied, there is a large sparse linear system to be solved at each time step. In this chapter, we introduce this discretization method for the two-asset Black-Scholes problem. Furthermore the numerical method to American type two-asset options is also discussed.

## 4.1 General Two-Asset Black-Scholes PDE

Recall that the two-asset Black-Scholes PDE is given by

$$\frac{\partial u}{\partial t} + \frac{1}{2}\sigma_1^2 S_1^2 \frac{\partial^2 u}{\partial S_1^2} + \frac{1}{2}\sigma_2^2 S_2^2 \frac{\partial^2 u}{\partial S_2^2} + \rho\sigma_1\sigma_2 S_1 S_2 \frac{\partial^2 u}{\partial S_1 \partial S_2} + rS_1 \frac{\partial u}{\partial S_1} + rS_2 \frac{\partial u}{\partial S_2} - ru = 0 \tag{4.1}$$

where $t \in [0, T]$.
In order to make it convenient for numerical PDE methods, we apply a variable transformation $\tau = T - t$ in the time dimension. The variable $\tau$ can be seen as the backward time which is the time left to the maturity. Therefore, the Black-Scholes equation becomes

$$\frac{\partial u}{\partial \tau} = \frac{1}{2}\sigma_1^2 S_1^2 \frac{\partial^2 u}{\partial S_1^2} + \frac{1}{2}\sigma_2^2 S_2^2 \frac{\partial^2 u}{\partial S_2^2} + \rho\sigma_1\sigma_2 S_1 S_2 \frac{\partial^2 u}{\partial S_1 \partial S_2} + rS_1 \frac{\partial u}{\partial S_1} + rS_2 \frac{\partial u}{\partial S_2} - ru \tag{4.2}$$

where $\tau \in [0, T]$. The final condition of (4.1) is the initial condition of (4.2).
Let's define the two-asset Black-Scholes operator

$$L \equiv \frac{1}{2}\sigma_1^2 S_1^2 \frac{\partial^2}{\partial S_1^2} + \frac{1}{2}\sigma_2^2 S_2^2 \frac{\partial^2}{\partial S_2^2} + \rho\sigma_1\sigma_2 S_1 S_2 \frac{\partial^2}{\partial S_1 \partial S_2} + rS_1 \frac{\partial}{\partial S_1} + rS_2 \frac{\partial}{\partial S_2} - r \tag{4.3}$$

and the two-asset Black-Scholes PDE becomes

$$\frac{\partial u}{\partial \tau} = Lu \tag{4.4}$$

In this chapter, we stick with (4.2) or (4.4) as Black-Scholes equation with payoff function as initial conditions.

## 4.2 Discretization

First, we need to discretize the PDE (4.2) or (4.4). In numerically solving parabolic PDEs such as Black-Scholes PDE using FDMs, the space dimension(s) and the time dimension are handled differently.

### 4.2.1 Space Discretization

The space domain for Black-Scholes PDE is semi-infinite, $[0, \infty) \times [0, \infty)$. However, for computational purposes, we truncate the domain to $[0, S_{1,\infty}] \times [0, S_{2,\infty}]$, for appropriately large $S_{1,\infty}$ and $S_{2,\infty}$.

Although our space domain here consists of two dimensions representing the two asset prices $S_1$ and $S_2$, we start the introduction of the discretization method on a one-dimensional space domain.

### Uniform Space Discretization

Suppose the domain $[a, b]$ is divided into equal-length $N$ subintervals. The mesh size is $h = \frac{b-a}{N}$ and the grid points are $S_i = ih + a$, where $i = 0, 1, 2, \ldots, N$. Suppose the function value $u(S_i)$ is denoted as $u_i$.


Figure 4.1: A uniform grid.

A finite difference approximation to the second derivative at point $S_i$ is given by

$$\frac{\partial^2 u_i}{\partial S^2} = \frac{1}{h^2}u_{i-1} - \frac{2}{h^2}u_i + \frac{1}{h^2}u_{i+1} + O(h^2), \tag{4.5}$$

and referred to as center difference approximation to the second derivative, while some finite difference approximations to the first derivative at point $S_i$ are

$$\frac{\partial u_i}{\partial S} = -\frac{1}{2h}u_{i-1} + \frac{1}{2h}u_{i+1} + O(h^2) \qquad \text{centered difference,} \tag{4.6}$$

$$\frac{\partial u_i}{\partial S} = -\frac{1}{h}u_i + \frac{1}{h}u_{i+1} + O(h) \qquad \text{forward difference,} \tag{4.7}$$

$$\frac{\partial u_i}{\partial S} = -\frac{1}{h}u_{i-1} + \frac{1}{h}u_i + O(h) \qquad \text{backward difference.} \tag{4.8}$$

Here the terms $O(h^k)$ are the truncation errors. The notation $O(h^k)$ means $O(h^k) = a_1h^k + a_2h^{k+1} + \cdots \leq (a_1 + a_2 + \ldots)h^k$ since $h$ is always small as $N \to \infty$. In the finite difference approximation (4.5) and (4.6), the leading order terms in truncation errors are proportional to $h^2$. Then we say the approximations have second order accuracy. At the same time, the finite difference approximations in equations (4.7) and (4.8) have first order accuracy. In most of the cases, the higher the order of the approximation is, the more accurate it is under the same mesh refinement. Therefore, for the approximation of $\frac{\partial u_i}{\partial S}$, we choose centered difference.

By (4.5), the vector of values of the second derivatives $\frac{\partial^2 u}{\partial S^2}$ at the grid points $S_i$, $i = 1, \ldots, N-1$, gives rise to $T_2\hat{u} + b_2$ where

$$T_2 = \frac{1}{h^2}\begin{bmatrix} -2 & 1 & & & \\ 1 & -2 & 1 & & \\ & & \ddots & & \\ & & 1 & -2 & 1 \\ & & & 1 & -2 \end{bmatrix}, \hat{u} = \begin{bmatrix} \hat{u_1} \\ \hat{u_2} \\ \vdots \\ \hat{u_{N-2}} \\ \hat{u_{N-1}} \end{bmatrix}, b_2 = \begin{bmatrix} \hat{u_0}/h^2 \\ 0 \\ \vdots \\ 0 \\ \hat{u_N}/h^2 \end{bmatrix}$$

where $\hat{u}_i \approx u(S_i)$.

By (4.6), the vector of values of the first derivative $\frac{\partial u}{\partial S}$ at the grid points $S_i$, $i = 1, \ldots, N-1$, gives rise to $T_1\hat{u} + b_1$ where

$$T_1 = \frac{1}{2h}\begin{bmatrix} 0 & 1 & & & \\ -1 & 0 & 1 & & \\ & & \ddots & & \\ & & -1 & 0 & 1 \\ & & & -1 & 0 \end{bmatrix}, \hat{u} = \begin{bmatrix} \hat{u_1} \\ \hat{u_2} \\ \vdots \\ \hat{u_{N-2}} \\ \hat{u_{N-1}} \end{bmatrix}, b_1 = \begin{bmatrix} -\hat{u_0}/2h \\ 0 \\ \vdots \\ 0 \\ \hat{u_N}/2h \end{bmatrix}$$

The discretization matrices $T_1$ and $T_2$ are tridiagonal.

### Non-Uniform Space Discretization

It is not always the cases that the grid points should be equally spaced. In practice, different problems may need different space discretization mostly depending on the shape of the solutions. In the option pricing problem, we prefer to use non-uniform space discretization. Here are some reasons why we prefer non-uniform discretization in space for option pricing problem:

- The initial conditions (pay-off functions) are not smooth functions. The errors around the points of non-smoothness are expected to be larger. Therefore we need more grid points in these areas to increase the accuracy.

- In some parts of domain, the solution is close to linear. Therefore sparser grid points will still maintain a good approximation in these areas.

- Not all parts of domain are equally interesting to us. For example, if the stock prices now (spot prices) are $S_1 = 100$ and $S_2 = 100$, it is very unlikely to reach $S_1 = 800$ and $S_2 = 800$ in the stock market in the near future. Therefore in option pricing, we care more about a particular area of asset prices which are close to the spot prices. We refer to this area as *spotting area*. We set more grid points in that area.

Suppose the domain $[a, b]$ is divided into $N$, not necessarily equal-length, subintervals. The grid points are $S_i$, where $i = 0, 1, 2, \ldots, N$, with $S_0 = a$ and $S_N = b$ and the mesh sizes are $h_i = S_i - S_{i-1}$ where $i = 1, 2, \ldots, N$.
Then the centered difference approximation of the second derivative with respect to $S$ is

given by

$$\frac{\partial^2 u_i}{\partial S^2} = \frac{2}{h_i(h_i+h_{i+1})}u_{i-1} + \frac{-2}{h_i h_{i+1}}u_i + \frac{2}{(h_i+h_{i+1})h_{i+1}}u_{i+1} + O(h_i - h_{i+1}) + O(\max(h_i^2, h_{i+1}^2)). \quad (4.9)$$

From (4.9), we notice that the approximation may not maintain the second order accuracy because of the term $O(h_i - h_{i+1})$. However, if our non-uniform discretization is generated from a smooth mapping function, it can be proved that $O(h_i - h_{i+1}) \approx O(h^2)$ where $h$ is the mesh size of uniform discretization. More specifically, suppose $x_i = a + ih$, $i = 0, \ldots, N$, and $h = \frac{b-a}{N}$. Let $w(x)$ be a strictly increasing smooth-enough function with $w(a) = a$ and $w(b) = b$. Let $S_i = w(x_i)$, $i = 0, \ldots, N$. Then

$$\begin{aligned} h_i - h_{i+1} &= 2S_i - S_{i-1} - S_{i+1} \\ &= 2w(x_i) - w(x_i - h) - w(x_i + h) \\ &= 2w(x_i) - (w(x_i) - hw'(x_i) + \frac{h^2}{2}w''(x_i) + O(h^3)) \\ &\quad - (w(x_i) + hw'(x_i) + \frac{h^2}{2}w''(x_i) + O(h^3)) \\ &= -h^2 w''(x_i) - O(h^3) = O(h^2). \end{aligned}$$

Therefore, the truncation error term of (4.9) still has second order of convergence if a smooth mapping is used to generate the non-uniform grid points.

The centered-order approximation to the first derivative with respect to $S$ is given by

$$\frac{\partial u_i}{\partial S} = \frac{-h_{i+1}}{h_i(h_i+h_{i+1})}u_{i-1} + \frac{h_{i+1}-h_i}{h_i h_{i+1}}u_i + \frac{h_i}{(h_i+h_{i+1})h_{i+1}}u_{i+1} + O(h_i h_{i+1}), \quad (4.10)$$

and is second-order.

### Non-Uniform Mappings

Smooth mappings of uniform to non-uniform grid points are used to generate the needed non-uniform discretization. In this section, two non-uniform mappings, which are mainly used in option pricing problems are introduced.
Suppose $a = 0$. Thus the domain is $[0, b]$

1. The first mapping is given by

$$S_i = w(x_i) = \frac{(1+\eta)^{x_i/x_N} - 1}{\eta} b. \tag{4.11}$$

This mapping produces denser grid points towards zero. Larger parameter $\eta$ increases the density of the points towards zero.

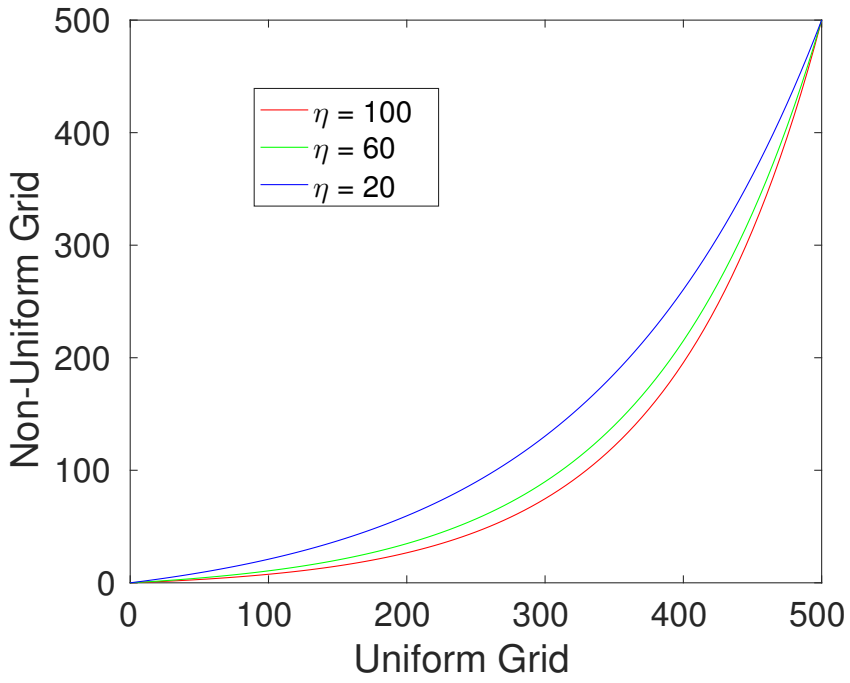


Figure 4.2: Plot of non-uniform grid points generated by (4.11) versus uniform grid points.

2. The second mapping is given by

$$S_i = w(x_i) = (1 + \frac{\sinh(\beta - (x_i/x_N - \alpha))}{\sinh(\beta\alpha)})E \tag{4.12}$$

This mapping produces denser grid points around $E$. Larger parameter $\alpha$ increases the density of the points. The purpose of parameter $\beta$ is to ensure the last grid point is $b$.

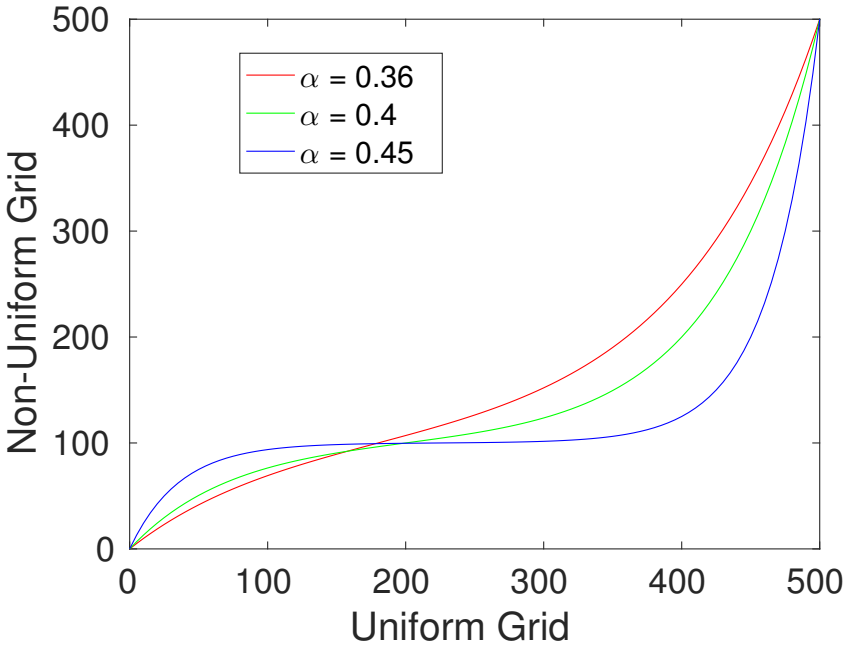


Figure 4.3: Plot of non-uniform grid points generated by (4.12) with $E = 100$ versus uniform grid points.

### Space Discretization of $Lu$

Now we can start to derive the discretization for $Lu$. Suppose the non-uniform partition of first asset price domain $[0, S_{1,\infty}]$ is $0 = S_{1,0} < S_{1,1} < \cdots < S_{1,N_1} = S_{1,\infty}$ and non-uniform partition of second asset price domain $[0, S_{2,\infty}]$ is $0 = S_{2,0} < S_{2,1} < \cdots < S_{2,N_1} = S_{2,\infty}$. Let $h_{1,i} = S_{1,i+1} - S_{1,i}$ where $i = 1, 2, \ldots, N_1$ and $h_{2,i} = S_{2,i+1} - S_{2,i}$ where $i = 1, 2, \ldots, N_2$. Assume Dirichlet conditions are used.

Assume $T_{2,S_1}$ is the discretization matrix of $\frac{\partial^2}{\partial S_1^2}$ on the dimension of $S_1$, $T_{1,S_1}$ is the discretization matrix of $\frac{\partial}{\partial S_1}$ on the dimension of $S_1$, $\mathbf{I}_{S_1}$ is the discretization matrix representing identity operator on the dimension of $S_1$, $T_{2,S_2}$ is the discretization matrix of $\frac{\partial^2}{\partial S_2^2}$ on the dimension of $S_2$, $T_{1,S_2}$ is the discretization matrix of $\frac{\partial}{\partial S_2}$ on the dimension of $S_2$ and $\mathbf{I}_{S_2}$ is the discretization matrix representing identity operator on the dimension of $S_2$.

The matrix $\mathbf{I}_{S_1}$ is identity matrix with order $(N_1 - 1)$ while $\mathbf{I}_{S_2}$ is identity matrix with order $(N_2 - 1)$. The matrices $T_{2,S_1}$ and $T_{1,S_1}$ are tridiagonal matrices with size $(N_1 - 1) \times (N_1 - 1)$ while the matrices $T_{2,S_2}$ and $T_{1,S_2}$ are tridiagonal matrices with size $(N_2 - 1) \times (N_2 - 1)$. The discretization matrix in higher dimension can be obtained by tensor product of discretization matrices from lower dimension.

**Definition.** The **tensor product** $A \otimes B$ of two matrices $A$ and $B$ is also called **Kro-**

**necker product** of two matrices. If $A$ is an $m \times n$ matrix and $B$ is a $p \times q$ matrix, then the Kronecker product $A \otimes B$ is the $mp \times nq$ block matrix defined by:

$$A \otimes B = \begin{bmatrix} a_{11}B & \dots & a_{1n}B \\ \vdots & \ddots & \vdots \\ a_{m1}B & \dots & a_{mn}B \end{bmatrix}. \tag{4.13}$$

Then the discretization matrix $A$ of the two-asset Black-Scholes operator $L$ can be written as $A = C_{2,0}A_{2,0} + C_{0,2}A_{0,2} + C_{1,1}A_{1,1} + C_{1,0}A_{1,0} + C_{0,1}A_{0,1} + C_{0,0}A_{0,0}$ where

$$A_{2,0} = T_{2,S_1} \otimes \mathbf{I}_{S_2} \tag{4.14}$$
$$A_{0,2} = \mathbf{I}_{S_1} \otimes T_{2,S_2} \tag{4.15}$$
$$A_{1,1} = T_{1,S_1} \otimes T_{1,S_2} \tag{4.16}$$
$$A_{1,0} = T_{1,S_1} \otimes \mathbf{I}_{S_2} \tag{4.17}$$
$$A_{0,1} = \mathbf{I}_{S_1} \otimes T_{1,S_2} \tag{4.18}$$
$$A_{0,0} = \mathbf{I}_{S_1} \otimes \mathbf{I}_{S_2}. \tag{4.19}$$

and where the coefficient matrices $C_{*,*}$ are defined further below. The tensor products also give us the ordering of the grid points. Suppose $\hat{u}$ is the approximate solution vector of ordered grid points. Then grid point $(S_{1,i}, S_{2,j})$ is the $k = ((i-1)(N_2-1)+j)$-th grid point. So $\hat{u}_k \approx u(S_{1,i}, S_{2,j})$. The coefficient matrices $C_{*,*}$ are all diagonal matrices where

$$C_{2,0} = \frac{\sigma_1^2}{2}\mathbf{diag}\{S_{1,1}^2, S_{1,2}^2, \dots, S_{1,N_1-1}^2\} \otimes \mathbf{I}_{S_2}, \tag{4.20}$$
$$C_{0,2} = \frac{\sigma_2^2}{2}\mathbf{I}_{S_1} \otimes \mathbf{diag}\{S_{2,1}^2, S_{2,2}^2, \dots, S_{2,N_2-1}^2\}, \tag{4.21}$$
$$C_{1,1} = \rho\sigma_1\sigma_2\mathbf{diag}\{S_{1,1}, S_{1,2}, \dots, S_{1,N_1-1}\} \otimes \mathbf{diag}\{S_{2,1}, S_{2,2}, \dots, S_{2,N_2-1}\}, \tag{4.22}$$
$$C_{1,0} = r\mathbf{diag}\{S_{1,1}, S_{1,2}, \dots, S_{1,N_1-1}\} \otimes \mathbf{I}_{S_2}, \tag{4.23}$$
$$C_{0,1} = r\mathbf{I}_{S_1} \otimes \mathbf{diag}\{S_{2,1}, S_{2,2}, \dots, S_{2,N_2-1}\}, \tag{4.24}$$
$$C_{0,0} = -r\mathbf{I}_{S_1} \otimes \mathbf{I}_{S_2}, \tag{4.25}$$

and $\mathbf{diag}\{a_1, a_2, \dots, a_n\}$ means a diagonal matrix with $a_i$, $i = 1, \dots, n$, as $i^{th}$ diagonal element.

The arising matrix $A$ is block tridiagonal matrix with size $(N_1-1)(N_2-1) \times (N_1-1)(N_2-1)$. Note also that $A_{0,0} = \mathbf{I}$ where $\mathbf{I}$ is identity matrix of order $(N_1-1)(N_2-1)$.

### 4.2.2 Time Discretization

After applying the space discretization, we have transformed equation $\frac{\partial u}{\partial \tau} = Lu$ into a system of ordinary differential equations (ODEs) with $(N_1 - 1)(N_2 - 1)$ unknowns $\hat{u}(\tau, S_{1,i}, S_{2,j})$, $i = 1, \ldots, N_1 - 1$ and $j = 1, \ldots, N_2 - 1$. Our system of ODEs is

$$\frac{\partial \hat{u}}{\partial \tau} = A\hat{u} + b \tag{4.26}$$

where $\hat{u}$ the approximate solution vector of components $\hat{u}(\tau, S_{1,i}, S_{2,j})$ with the ordering explained before and $b$ is the vector that combines the boundary conditions and the source function. However, in Black-Scholes equation, the source function on the right-hand-side of equation is zero, therefore the vector $b$ only contains contributions from the boundary conditions.

In order to solve (4.26) numerically, firstly let $\tau^k$, $k = 0, 1, \ldots, N_t$ be discretization on the time dimension $[0, T]$ with $0 = \tau^0 < \tau^1 < \cdots < \tau^{N_t} = T$ and the time-step $\Delta\tau^k = \tau^k - \tau^{k-1}$ where $k = 1, \ldots, N_t$. Note that these time points may not be equally spaced. We denote by $\hat{u}^k$ the numerical solution vector of components $\hat{u}(\tau^k, S_{1,i}, S_{2,j})$, and by $b^k$ the vector containing contributions from the boundary conditions at time $\tau^k$.

The $\theta$-time-stepping scheme from time $\tau^{k-1}$ to time $\tau^k$ can be written as

$$\frac{\hat{u}^k - \hat{u}^{k-1}}{\Delta\tau^k} = \theta A\hat{u}^k + \theta\hat{b}^k + (1-\theta)A\hat{u}^{k-1} + (1-\theta)\hat{b}^{k-1} \tag{4.27}$$

$$\Longrightarrow (\mathbf{I} - \theta\Delta\tau^k A)\hat{u}^k = (\mathbf{I} + (1-\theta)\Delta\tau^k A)\hat{u}^{k-1} + \Delta\tau^k(\theta\hat{b}^k + (1-\theta)\hat{b}^{k-1}). \tag{4.28}$$

In (4.27) and (4.28), the parameter $\theta \in [0, 1]$ may take the following values giving rise to the respective schemes

- $\theta = 0$, the forward (fully explicit) Euler Scheme,
- $\theta = 1$, the backward (fully implicit) Euler Scheme,
- $\theta = \frac{1}{2}$, the Crank-Nicolson (CN) scheme.

It is well-known that the CN scheme has second-order accuracy in the time dimension while the forward Euler and the backward Euler schemes have first-order accuracy. Therefore, we mainly use the CN scheme. However, we notice that the initial condition of Black-Scholes equation is not smooth function which may produce spurious oscillations around the non-smoothness. Because the fully implicit scheme has stronger stability property, in order to help the CN scheme maintain a good stability, the *Rannacher smoothing* [16] technique is suggested. The Rannacher smoothing uses the fully-implicit

time-stepping in the first few time-steps with smaller time-step size, and then switches back to CN scheme. In the experiments, we find this helps to smoothen the discontinuity of the first derivatives of the pay-off.

## 4.3 Penalty Method for American Options

Similarly as for the one-asset American option, the two-asset American option price can never go below the pay-off. Therefore, that the two-asset American option pricing problem can also be written in the form of LCP as

$$\left\{ \begin{array}{r} \frac{\partial u}{\partial \tau} - Lu = 0 \\ u - f \geq 0 \end{array} \right\} \vee \left\{ \begin{array}{r} \frac{\partial u}{\partial \tau} - Lu \geq 0 \\ u - f = 0 \end{array} \right\} \tag{4.29}$$

where $\frac{\partial u}{\partial \tau} - Lu = 0$ is two-asset Black-Scholes equation and $f(S_1, S_2) = u(0, S_1, S_2)$ is the pay-off function (initial condition).

As in the one-asset American option case, equation (4.3) divided the domain into two sets and the unknown boundary which separates the two regions is called *free boundary*. We note that at each time $\tau$, the free boundary in the one-asset American option is a point, while in the two-asset American option it is a line.

In 2008, Forsyth and Vetzal [6] proposed the discrete penalty method to numerically solve the LCP arising from one-asset American options. They replace (4.3) by a non-linear PDE by adding a positive penalty term to the right hand side of the Black-Scholes equation. The resulting PDE can be written as

$$\frac{\partial u}{\partial \tau} - Lu = p \max(f - u, 0) \tag{4.30}$$

where the $p$ is a large positive penalty factor. The penalty forces the solution of (4.30) to approximately satisfy the free boundary condition $u \geq f$. More specifically, when $p \to +\infty$, the solution of (4.30) converges to the exact solution of the LCP by satisfying $u \geq f - \epsilon$ for $\epsilon \sim O(\frac{1}{p})$.

### Penalty Term Discretization

The space discretization method for $Lu$ and time-stepping method for (4.30) are exactly same as for (4.4). We now discuss the treatment of the penalty term $p \max(f - u, 0)$ in (4.30). When calculating the numerical solution $\hat{u}^k$ from time $\tau^{k-1}$ to $\tau^k$, the penalty term is discretized as $P(\hat{u}^k)(\hat{f} - \hat{u}^k)$ where $\hat{f}$ is the vector of pay-off function values at

grid points and $P(\hat{u}^k)$ is a diagonal matrix defined as

$$[P(\hat{u}^k)]_{i,i} \equiv \begin{cases} p & \text{if } (\hat{u}^k)_i < (\hat{f})_i, \\ 0 & \text{otherwise.} \end{cases} \tag{4.31}$$

Therefore when adding the discrete penalty term to linear system (4.28), at each time-step, the arising system is

$$\begin{aligned}(\mathbf{I} - \theta\Delta\tau^k A)\hat{u}^k + P(\hat{u}^k)\hat{u}^k = (\mathbf{I} + (1-\theta)\Delta\tau^k A)\hat{u}^{k-1} \\ +\tau^k(\theta\hat{b}^k + (1-\theta)\hat{b}^{k-1}) + P(\hat{u}^k)\hat{f}.\end{aligned} \tag{4.32}$$

For this time-step, only $\hat{u}^k$ is unknown and needs to be computed. However, there is a non-linearity between $P(\hat{u}^k)$ and $\hat{u}^k$. Forsyth and Vetzal use Newton's iteration to solve (4.32). The large penalty factor $p$ is chosen as

$$p \approx \frac{1}{tol} \tag{4.33}$$

where *tol* is the tolerance for the stopping criterion for Newton's iteration.

### Penalty Iteration

Newton's Iteration method to solve (4.32) at each time-step is often called discrete penalty iteration for American option pricing. For simplicity, we assume $Q^k = (\mathbf{I} - \theta\Delta\tau^k A)$ and $g^k = (\mathbf{I} + (1-\theta)\Delta\tau^k A)\hat{u}^{k-1} + \tau^k(\theta\hat{b}^k + (1-\theta)\hat{b}^{k-1})$.

**Algorithm 1** Penalty iteration to compute $\hat{u}^k$ given $\hat{u}^{k-1}$

**Require:** solve $(Q^k + P(\hat{u}^k))\hat{u}^k = g^k + P(\hat{u}^k)\hat{f}$

1: $\hat{u}^{k,0} = \hat{u}^k$ (Initialization)
2: **for** $m = 1, 2, \ldots$ **do**
3: solve $(Q^k + P(\hat{u}^{k,m-1}))\hat{u}^{k,m} = g^k + P(\hat{u}^{k,m-1})\hat{f}$
4: **if** $\frac{\|\hat{u}^{k,m} - \hat{u}^{k,m-1}\|}{\max\{1, \|\hat{u}^{k,m}\|\}} \leq tol$ or $P(\hat{u}^{k,m}) = P(\hat{u}^{k,m-1})$ **then**
5: break;
6: **end if**
7: **end for**
8: $\hat{u}^k = \hat{u}^{k,m}$

## 4.4 Special Considerations

### PDE Boundary Conditions

As mentioned before, besides the Dirichlet boundary condition, PDE boundary conditions are also considered for Exchange options and Spread options on the far-side boundaries. The reason is that, on the truncated far-side boundary, the points still satisfy the two-asset Black-Scholes equation

$$\frac{\partial u}{\partial t} = Lu. \tag{4.34}$$

In order to apply the PDE boundary conditions, we discretize (4.34) on the boundary points and incorporate the resulting equations into the system (4.28). On the far-side boundaries, we use the first-order difference scheme to discretize the derivatives. The discretization matrix of two-dimensional space can also be obtained by tensor products similarly as (4.14) - (4.19). Therefore, only the first order difference method in one dimension will be discussed here. Assume $S_i$, $i = 0, 1, 2, \ldots, N$, with $S_N = S_\infty$, are the grid points and the mesh sizes are $h_i = S_i - S_{i-1}$ where $i = 1, 2, \ldots, N$. Then the first order difference scheme on the boundary point $S_N$ is

$$\begin{aligned}\frac{\partial^2 u_N}{\partial S^2} = &\frac{2}{h_{N-1}(h_N + h_{N-1})}u_{N-2} + \frac{-2}{h_N h_{N-1}}u_{N-1} + \frac{2}{(h_N + h_{N-1})h_N}u_N \\ &+ O(\frac{h_N^2}{h_{N-1}}) + O(\frac{(h_N + h_{N-1})^2}{h_{N-1}})\end{aligned} \tag{4.35}$$

$$\frac{\partial u_N}{\partial S} = \frac{1}{h_N}u_N - \frac{1}{h_N}u_{N-1} + O(h_N) \tag{4.36}$$

From numerical experiments, it can be shown that the first order approximation on the PDE boundaries does not affect the second order of convergence of the absolute error in the spotting area, even if theoretically the complete difference scheme is first order.

After applying tensor products to get the discretization matrices in the two-dimensional space domain, with the PDE boundary conditions, the matrix $A$ in equation (4.28) is of size $N_1N_2 \times N_1N_2$. The discretized solution vector $\hat{u}$ has length $N_1N_2$ because it contains the values on the grid points far-side boundaries.

### Exchange Options

The choice of non-uniform mapping is important to obtain an accurate numerical solution. In Exchange option, the pay-off (initial conditions) function is not smooth along the line

when $S_1 = S_2$. In this case, ideally we want to push more grid points to this line first. However, this is not possible with a rectangular grid. In our experiments, we have used the two-mapping functions (4.11) and (4.12) in both dimensions.

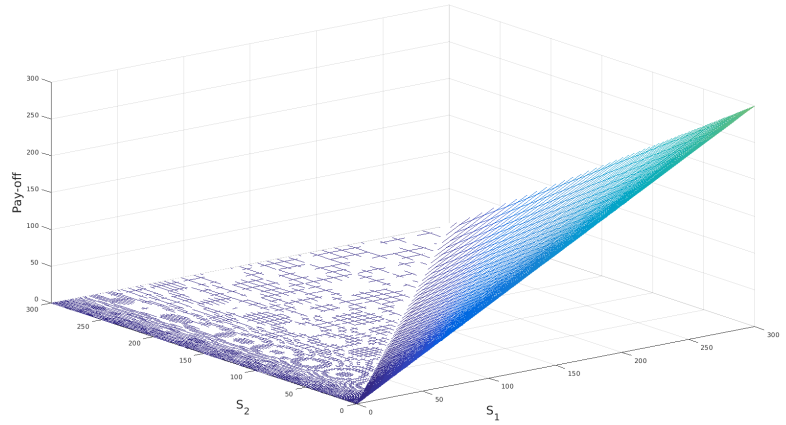


Figure 4.4: Pay-off of Exchange option.

The non-uniform discretization generated from the first non-uniform mapping (4.11) pushes more grid points towards the origin. Therefore it can give us accurate numerical solution for points closed to the origin. This non-uniform mapping will push more grid points towards the origin. We set the parameter of (4.11) to $\eta = 80$.

The second non-uniform mapping (4.12) can help to push more grid points towards the spotting area. Therefore, the non-uniform discretization generated by (4.12) can give us more accurate numerical solution in the spotting area. The parameter $E$ is often set as the spot price in each dimension. We set the parameter $\alpha$ of (4.13) to $\alpha = 0.36$ in both dimensions.

### Spread Options

In Spread call option, the pay-off (initial conditions) function is not smooth along the line when $S_1 = S_2 + K$. In this case, we want to push more grid points to this line.

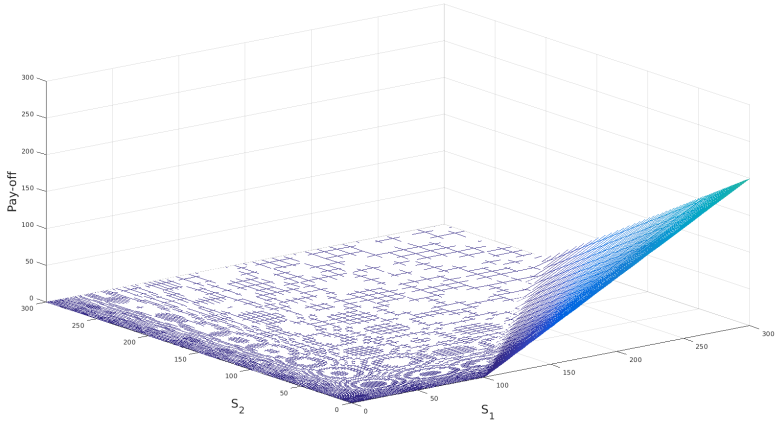


Figure 4.5: Pay-off of Spread option with Strike $K = 100$.

Again this is not possible with a rectangular grid. In Spread option, we mostly apply the second non-uniform mapping (4.12) on the two space dimensions. Therefore, we can obtain an accurate numerical solutions in the spotting area.

## 4.5 Iterative Methods for solving Linear Systems

At each timestep of the CN method applied to the two-asset Black-Scholes PDE, a large sparse linear system needs to be solved. The size of this linear system is approximately $N_1N_2$. If we increase the number of subintervals in the $S_1$ and $S_2$ dimensions from $N_1$ and $N_2$ to $2N_1$ and $2N_2$, respectively, the size of matrices increases from $N_1N_2$ to $4N_1N_2$. Furthermore, the bandwidth of the matrices increases from $N_2$ to $2N_2$. Therefore, the computational cost of a standard direct linear solver (e.g. LU factorization by Gaussian Elimination with or without pivoting) increases from $N_2^3N_1$ to $8N_2^3N_1$. In order to avoid this high computational cost, we choose to apply an iterative method for the solution of the linear system at each timestep.

This chapter describes iterative methods with preconditioning techniques for solving the arising linear system during each timestep from the CN timestepping scheme. Our approach is to use the restarted Generalized Minimal Residual method (GMRES(restart)) with incomplete LU (ILU) factorization preconditioning.

### 4.5.1 GMRES with a ILU Preconditioning

Recall from (4.28) that the CN scheme at each timestep solves a linear system with matrix $(\mathbf{I} - \theta\Delta\tau^k A)$. To solve this linear system, GMRES is used, because the matrix

$\mathbf{I} - \theta\Delta\tau^k A$ is non-symmetric and non-positive-definite. In this case, some commonly used iterative methods, such as successive over-relaxation (SOR) or Conjugate Gradient method (CG), do not guarantee convergence. The GMRES method was introduced in [18] and more details about various versions of it can be found in [17].

A good choice of initial guess can accelerate the convergence of an iterative method. In our problem, the initial guess for GMRES is usually constructed by linear extrapolation of the numerical solutions of the previous two timesteps except the first timestep. During the first timestep, we use the initial condition as the initial guess of GMRES.

The choice of preconditioner is critical for the convergence of the iterative method. We choose to use the ILU preconditioner [17] which means that the preconditioning matrix $P$ is obtained from an ILU factorization of $\mathbf{I} - \theta\Delta\tau^k A$.

Another possible choice of preconditioner for the matrix $\mathbf{I} - \theta\Delta\tau^k A$ is the matrix arising from the discretization of

$$\frac{\partial u}{\partial \tau} = \triangle u \tag{4.37}$$

with CN scheme, where $\triangle$ is the Laplacian operator. The advantage of this preconditioner is that the matrix $P$ can be fast and directly solved by fast Fourier transform (FFT) techniques. However, the Fourier-based solver often requires uniform step-size, while for our numerical methods, we prefer to use non-uniform discretization on the space domain. Therefore, we choose to use the ILU preconditioner which is more general and flexible.

An ILU factorization of a matrix is a sparse approximation of the LU factorization. A standard LU factorization applied to $Ax = b$ will cause fill-in, in which case new non-zero entries will be introduced, and the sparsity of LU factors is reduced compared to that of the original matrix, which increases the floating-point operation counts and the memory requirements. In ILU, we commonly restrict the fill-in to either zero entries or few entries and find the lower triangular matrix $\tilde{L}$ and upper triangular matrix $\tilde{U}$ such that $A \approx P = \tilde{L}\tilde{U}$. Since the matrix $P$ is already factored into sparse factors, it can be easily solved and it is a good choice for preconditioner of matrix $A$ in an iterative method.

Regarding the ILU factorization algorithm, we have considered two versions. First is the *no-fill* version, which does not allow any fill-in at all. In this case, the matrix $P$ has the same sparsity pattern as $A$. Second is the *drop-tolerance* version, in which we usually set a threshold and ignore all fill-in entries that are above a certain value that depends on the threshold. In this case, $P$ is a little less sparse than $A$, but still very sparse. In our experiments, we test the efficiency of these two strategies on our problem.

We use the built-in **MATLAB** functions *GMRES* and *ILU* for implementation. The experimental results can be found in the next chapter.

## 4.6 Other Fast Solution Techniques

Another way to avoid the high computational cost of direct linear solver, applied to a large bandwidth linear system, is to use a timestepping technique other than CN. More specifically, Alternating Direction Implicit (ADI) timestepping methods result in solving multiple tridiagonal linear systems at each timestep. Thus the computational cost per timestep is proportional to the number of unknowns. However, in this project, we do not pursue this approach. As it will be shown, the ILU preconditioned GMRES results in complexity proportional to the number of unknowns.

# Chapter 5

# Numerical Experiments

In this chapter, numerical experiments are performed to explore the effectiveness of our numerical methods for solving the Black-Scholes PDE arising in pricing Exchange and Spread options. Even if we are more interested in pricing Spread options, European and American, we start by testing our numerical methods on European Exchange options. This is because for European Exchange options, there is an analytical formula giving the solution. In addition, Exchange options are special cases of Spread options, when $K = 0$. Therefore, we believe that the study of the effect of some numerical and problem parameters of the methods on Exchange options will be helpful for the case of Spread options too. Such numerical choices include the choice of non-uniform space discretization and the choice of boundary conditions. Problem parameter choices include the maturity time and the values of volatilities and correlation.

Recall that $N_1$ and $N_2$ are the number of subintervals in the $S_1$ and $S_2$ dimensions, respectively. In most of the experiments, $N_1$ and $N_2$ are the same, but in some experiments, they may be different. In this project, we use constant time-steps. We set the size of the time-step to $\frac{2}{N_1}$. In the numerical experiments, the units for $S_1$ and $S_2$ are the dollar, while, the unit of time dimension is the year. Therefore, if $S_1 = 100$, $S_2 = 50$ and $T = 0.5$, it means the first asset price is \$100, the second asset price is \$50 and the maturity time is half a year. In this sense, the interest rate is compounded yearly rate.

In addition to testing our numerical methods in approximating the option price, we are also interested in the performance of our methods in approximating the Greeks, essentially the Delta ($\Delta$) and the Gamma ($\Gamma$) associated with the option and underlying assets. Greeks are very important parameters for some practical applications such as hedging. In Spread or Exchange option, there are two associated assets $S_1$ and $S_2$.

Therefore, we define

$$\Delta_{S_1} = \frac{\partial u}{\partial S_1}, \qquad \Delta_{S_2} = \frac{\partial u}{\partial S_2}, \tag{5.1}$$

$$\Gamma_{S_1} = \frac{\partial^2 u}{\partial S_1^2}, \qquad \Gamma_{S_2} = \frac{\partial^2 u}{\partial S_2^2}. \tag{5.2}$$

The values of Greeks are approximated with centered difference approximations (4.9) and (4.10). In the experiments, we find that, even if the numerical approximation to the option price appears smooth and convergent with consistent order, oscillations may still appear in the Delta and Gamma especially around the non-smoothness points. Thus, testing the Greeks is necessary.

In testing the values of price and Greeks, we consider two cases: the values on one point (usually the spot price), and the values in a certain area around the spot price, which we refer to as *spotting area*.

In PDE discretization methods, the rate of convergence is a very important property. We need to check whether the numerically observed rate of convergence agrees with the theoretical one. To calculate the numerically observed order of convergence for the cases that an exact analytical solution is available (e.g. the case of European Exchange options), we conduct experiments with at least two numbers of subintervals $n_1$ and $n_2$ and calculate the respective errors $e_1$ and $e_2$ as infinity norms of the errors of all points in a certain area. Then the rate of convergence is approximated by

$$\text{Rate of convergence} = \frac{\log(e_2/e_1)}{\log(n_1/n_2)}. \tag{5.3}$$

For the cases that an exact analytical solution is not available (e.g. the case of Spread options), we conduct experiments with at least three numbers of subintervals $n_1$, $n_2$ and $n_3$ and calculate the respective values $u_1$, $u_2$ and $u_3$ on a set of points or on one point. When the values $u_1$, $u_2$ and $u_3$ are calculated on a set of points, we then calculate the changes $\text{change}_2 = \|u_1 - u_2\|$ and $\text{change}_3 = \|u_2 - u_3\|$, as infinity norms of differences of all points in a certain area. Then the rate of convergence is approximated by

$$\text{Rate of convergence} = \frac{\log(\text{change}_3/\text{change}_2)}{\log(n_2/n_3)}. \tag{5.4}$$

When the values $u_1$, $u_2$ and $u_3$ are calculated on one point, we then calculate the changes $\text{change}_2 = u_1 - u_2$ and $\text{change}_3 = u_2 - u_3$. Then the rate of convergence is approximately

by

$$\text{Rate of convergence} = \frac{\log(|\text{change}_3/\text{change}_2|)}{\log(n_2/n_3)}. \tag{5.5}$$

Another important property in discretization methods for parabolic PDEs is stability. We calculate the spectral radius of the iteration matrix $(\mathbf{I}-\theta\Delta\tau^k A)^{-1}(\mathbf{I}+(1-\theta)\Delta\tau^k A)$ which gives information on the stability of the method. We also calculate the matrix condition number associated with the pricing problems, i.e. the condition number of the matrix $\mathbf{I}-\theta\Delta\tau^k A$ appearing in (4.28).

## 5.1 European Exchange Option

In this section, we test the effectiveness of different non-uniform discretizations of the spatial domain and the effectiveness of different boundary conditions. We also want to see how certain parameter settings affect the performance of our numerical methods.

For European Exchange options, we can use the analytical solution, given by the Margrabe formula [14] to calculate the infinity norm of the price errors on the spotting area and associated convergence rates for our numerical methods. The errors of the Greeks in spotting area are calculated by differentiating the Margrabe formula.

### 5.1.1 Different Space Discretizations

In our numerical method, it is mentioned that the uniform space discretization may not be a good choice for Black-Scholes-like PDE mainly because of the non-smoothness of initial condition. We have also introduced two non-uniform mappings to generate non-uniform space discretizations. Therefore, we need to test the performance of these three different space discretizations and appropriate parameter settings in our non-uniform mapping functions. In these experiments, to test different space discretizations, we use as basis the parameter settings shown in Table 5.1. For the boundary conditions, the Margrabe formula is used to generate the boundary values.

| Parameters | Value |
|---|---|
| Domain of $S_1$ | $[0, 500]$ |
| Domain of $S_2$ | $[0, 500]$ |
| Spot price | $S_1 = S_2 = 60$ |
| Spotting area | $[30, 180] \times [30, 180]$ |
| Time to maturity $T$ | 1 |
| Volatility of first asset $\sigma_1$ | 0.4 |
| Volatility of second asset $\sigma_2$ | 0.2 |
| Interest rate $r$ | 0.1 |
| Correlation $\rho$ | 0.4 |

Table 5.1: Model parameters for pricing European Exchange option

Tables 5.2, 5.3 and 5.4, and Figure 5.1a show results from pricing European Exchange option using uniform and two non-uniform grids. It can be seen that our numerical methods exhibit approximately second-order convergence in the spotting area. Among all the different space discretizations, we find that the non-uniform discretization generated from non-uniform mapping (4.11) gives the best result. This space discretization has the least error in the spotting area for both of the option value and Greeks. At the same time, the convergence rate with this space discretization is more stable even with only few grid points (25 or 50 grid points). For the other two space discretizations, the convergence rate oscillates when the grid sizes are not large enough. Furthermore, the benefits of the (4.11) non-uniform mapping are more prominant for the Gamma than for the price and Delta. As the number of grid points increases, the numerical methods show approximately second order of convergence for all grid discretizations.

In the case of Exchange option, we wish to set more grid points around non-smoothness line $S_1 = S_2$. Although the non-uniform mapping (4.11) actually pushes more grid points towards the origin, more grid points are also set close to the $S_1 = S_2$ line for small values of $S_1$ and $S_2$. However this non-uniform mapping may not be as effective in the Spread option case.

| $N_1, N_2$ | Value ($u$) | |
|---|---|---|
| | error | order |
| 25 | 1.17e+00 | |
| 50 | 2.32e-01 | 2.33 |
| 100 | 6.12e-02 | 1.92 |
| 200 | 1.61e-02 | 1.93 |
| 400 | 4.17e-03 | 1.95 |

| $N_1, N_2$ | $\Delta_{S_1}$ | | $\Gamma_{S_1}$ | | $\Delta_{S_2}$ | | $\Gamma_{S_2}$ | |
|---|---|---|---|---|---|---|---|---|
| | error | order | error | order | error | order | error | order |
| 25 | 4.97e-02 | | 2.48e-03 | | 1.31e-01 | | 1.89e-02 | |
| 50 | 1.25e-02 | 1.99 | 6.50e-04 | 1.93 | 1.61e-02 | 3.02 | 1.24e-03 | 3.93 |
| 100 | 3.57e-03 | 1.81 | 1.02e-04 | 2.67 | 5.51e-03 | 1.55 | 2.63e-04 | 2.23 |
| 200 | 1.03e-03 | 1.79 | 2.47e-05 | 2.05 | 1.67e-03 | 1.72 | 9.16e-05 | 1.53 |
| 400 | 2.76e-04 | 1.90 | 6.74e-06 | 1.87 | 4.58e-04 | 1.86 | 2.67e-05 | 1.78 |

Table 5.2: Numerical results (values and Greeks) for European Exchange option in spotting area with Margrabe boundary conditions. Settings in Table 5.1 and *uniform discretization* are used. The errors are calculated as infinity norms of errors of all grid points in the spotting area.

| $N_1, N_2$ | Value ($u$) | |
|---|---|---|
| | error | order |
| 25 | 8.95e-01 | |
| 50 | 2.17e-01 | 2.05 |
| 100 | 5.60e-02 | 1.95 |
| 200 | 1.40e-02 | 2.00 |
| 400 | 3.49e-03 | 2.00 |

| $N_1, N_2$ | $\Delta_{S_1}$ | | $\Gamma_{S_1}$ | | $\Delta_{S_2}$ | | $\Gamma_{S_2}$ | |
|---|---|---|---|---|---|---|---|---|
| | error | order | error | order | error | order | error | order |
| 25 | 1.37e-02 | | 3.69e-04 | | 1.41e-02 | | 3.80e-04 | |
| 50 | 3.44e-03 | 1.99 | 6.92e-05 | 2.41 | 3.58e-03 | 1.98 | 5.89e-04 | 2.69 |
| 100 | 8.89e-04 | 1.97 | 1.94e-05 | 1.84 | 9.25e-04 | 1.95 | 1.64e-05 | 1.84 |
| 200 | 2.22e-04 | 1.99 | 5.06e-06 | 1.94 | 2.33e-04 | 1.99 | 4.28e-06 | 1.94 |
| 400 | 5.57e-05 | 1.99 | 1.29e-06 | 1.97 | 5.86e-05 | 1.99 | 1.09e-06 | 1.97 |

Table 5.3: Numerical results (values and Greeks) for European Exchange option in spotting area with Margrabe boundary conditions. Settings in Table 5.1 and *non-uniform discretization* with mapping function (4.11) are used. In (4.11), parameter $\eta = 80$. The errors are calculated as infinity norms of errors of all grid points in the spotting area.

| $N_1, N_2$ | Value ($u$) | |
|---|---|---|
| | error | order |
| 25 | 1.99e+00 | |
| 50 | 4.38e-01 | 2.05 |
| 100 | 9.50e-02 | 1.95 |
| 200 | 2.14e-02 | 2.00 |
| 400 | 5.29e-03 | 2.00 |

| $N_1, N_2$ | $\Delta_{S_1}$ | | $\Gamma_{S_1}$ | | $\Delta_{S_2}$ | | $\Gamma_{S_2}$ | |
|---|---|---|---|---|---|---|---|---|
| | error | order | error | order | error | order | error | order |
| 25 | 2.79e-02 | | 2.31e-03 | | 7.40e-02 | | 2.30e-02 | |
| 50 | 5.47e-03 | 2.35 | 2.25e-04 | 3.36 | 4.90e-03 | 1.98 | 2.89e-04 | 5.29 |
| 100 | 1.18e-03 | 2.21 | 7.20e-05 | 1.65 | 1.81e-03 | 1.95 | 2.14e-04 | 1.46 |
| 200 | 2.72e-04 | 2.12 | 1.60e-05 | 2.17 | 4.18e-04 | 1.99 | 4.85e-05 | 2.14 |
| 400 | 6.61e-04 | 2.03 | 4.00e-06 | 2.00 | 1.06e-04 | 1.99 | 1.23e-05 | 1.98 |

Table 5.4: Numerical results (values and Greeks) for European Exchange option in spotting area with Margrabe boundary conditions. Settings in Table 5.1 and *non-uniform discretization* with mapping function (4.12) are used. In (4.12), parameter $\alpha \approx 0.36$ and $E = 60$. The errors are calculated as infinity norms of errors of all grid points in the spotting area.

### 5.1.2 Different Boundary Conditions

We have mentioned the importance of appropriate boundary conditions and presented three types of boundary conditions for Exchange option in Chapter 3. The numerical tests in this subsection show the effectiveness of these three types of boundary conditions. Furthermore, we need to compare the advantages and disadvantages of these three boundary conditions. In this subsection, we use the parameter settings shown in Table 5.1 and the non-uniform mapping (4.11) with $\eta = 80$.

Tables 5.2, 5.7 and 5.8 display the results for European Exchange option using Margrabe, pay-off and PDE boundary conditions, respectively. From Tables 5.2, 5.7 and 5.8, it is shown that there are minor differences in price in the spotting area. Theoretically, the Dirichlet boundary condition generated from Margrabe's formula should give us the best result in price. However, in practice, it seems that the PDE boundary conditions give slightly more accurate price. With Margrabe boundary condition, the approximations of the Greeks are accurate and stable with approximately second order of convergence. However, with PDE boundary conditions, the convergence of Greeks is not that stable. We will show (further in the thesis) that with PDE boundary conditions, some good

properties of the time-iteration matrix $(\mathbf{I}-\theta\Delta\tau^k A)^{-1}(\mathbf{I}+(1-\theta)\Delta\tau^k A)$ in (4.28) are lost.

From Table 5.5, we can see that, for Dirichlet boundary conditions such as pay-off or Margrabe, the spectral radius of the iterative matrix is less than 1 which ensures the stability of the numerical method for the parabolic PDE problem. Regarding the PDE boundary conditions, the spectral radius is above 1, in which case the stability may be an issue. However, because the spectral radius is only a little above 1, the numerical solution is still accurate if there are not too many time steps. At the same time, the spectral radius of PDE boundary conditions decreases with $N_1$ and seems to be approaching 1, while the spectral radius of Dirichlet boundary conditions increases with $N_1$ and seems to be approaching 1.

From Table 5.6, we find that all the matrices generated by Dirichlet BCs and PDE BCs are not ill-conditioned. However, we notice that the condition numbers of matrices are approximately linearly increasing with $N_1$. In this case, the matrices may become ill-conditioned only when the number of grid discretization points is extremely large which does not happen in practical cases, for the type of problem we are considering.

| $N_1, N_2$ | 25 | 50 | 100 | 200 |
|---|---|---|---|---|
| Dirichlet BCs | 0.9930 | 0.9932 | 0.9966 | 0.9983 |
| PDE BCs | 1.0080 | 1.0075 | 1.0036 | 1.0018 |

Table 5.5: Spectral radius of time-iteration matrix $(\mathbf{I}-\theta\Delta\tau^k A)^{-1}(\mathbf{I}+(1-\theta)\Delta\tau^k A)$ with different boundary conditions

| $N_1, N_2$ | 25 | 50 | 100 | 200 |
|---|---|---|---|---|
| Dirichlet BCs | 1.2775 | 2.1194 | 3.2396 | 5.4731 |
| PDE BCs | 3.4270 | 6.3010 | 14.7131 | 41.8457 |

Table 5.6: Condition number with respect to infinity norm of matrix $(\mathbf{I}-\theta\Delta\tau^k A)$ with different boundary conditions

Regarding the pay-off boundary conditions, we find that, compared to Margrabe boundary condition, the results of price and Greeks are only slightly worse but still acceptable. Stable order of convergence, approximately second order, is observed. Also, with respect to stability and conditioning, pay-off BCs behave as Margrabe boundary conditions. Therefore, pay-off boundary conditions are useful when exact solution formula is not available such as in the cases of Spread options or American type of options. In this cases, we will mainly use the pay-off boundary conditions.

| $N_1, N_2$ | Value ($u$) | |
|---|---|---|
| | error | order |
| 25 | 8.96e-01 | |
| 50 | 2.17e-01 | 2.05 |
| 100 | 5.63e-02 | 1.95 |
| 200 | 1.42e-02 | 1.99 |
| 400 | 3.72e-03 | 1.94 |

| $N_1, N_2$ | $\Delta_{S_1}$ | | $\Gamma_{S_1}$ | | $\Delta_{S_2}$ | | $\Gamma_{S_2}$ | |
|---|---|---|---|---|---|---|---|---|
| | error | order | error | order | error | order | error | order |
| 25 | 1.37e-02 | | 3.69e-04 | | 1.41e-02 | | 3.80e-04 | |
| 50 | 3.44e-03 | 1.99 | 6.92e-05 | 2.41 | 3.58e-03 | 1.98 | 5.89e-04 | 2.69 |
| 100 | 8.79e-04 | 1.97 | 1.94e-05 | 1.84 | 9.25e-04 | 1.95 | 1.64e-05 | 1.84 |
| 200 | 2.22e-04 | 1.99 | 5.06e-06 | 1.94 | 2.33e-04 | 1.99 | 4.28e-06 | 1.94 |
| 400 | 5.57e-05 | 1.99 | 1.29e-06 | 1.97 | 6.09e-05 | 1.94 | 1.09e-06 | 1.97 |

Table 5.7: Numerical results (values and Greeks) for European Exchange option in spotting area using *pay-off* boundary conditions. Settings in Table 5.1 and *non-uniform discretization* with mapping function (4.11) are used. The errors are calculated as infinity norms of errors of all grid points in the spotting area.

| $N_1, N_2$ | Value ($u$) | |
|---|---|---|
| | error | order |
| 25 | 8.95e-01 | |
| 50 | 2.15e-01 | 2.05 |
| 100 | 5.45e-02 | 1.98 |
| 200 | 1.31e-02 | 2.06 |
| 400 | 3.24e-03 | 2.01 |

| $N_1, N_2$ | $\Delta_{S_1}$ | | $\Gamma_{S_1}$ | | $\Delta_{S_2}$ | | $\Gamma_{S_2}$ | |
|---|---|---|---|---|---|---|---|---|
| | error | order | error | order | error | order | error | order |
| 25 | 1.37e-02 | | 3.69e-04 | | 1.41e-02 | | 3.80e-04 | |
| 50 | 3.44e-03 | 1.99 | 6.92e-05 | 2.41 | 3.58e-03 | 1.98 | 5.89e-04 | 2.69 |
| 100 | 8.79e-04 | 1.97 | 1.94e-05 | 1.84 | 9.25e-04 | 1.95 | 1.64e-05 | 1.84 |
| 200 | 2.22e-04 | 1.99 | 5.06e-06 | 1.94 | 2.33e-04 | 1.99 | 4.28e-06 | 1.94 |
| 400 | 5.57e-05 | 1.99 | 1.51e-06 | 1.74 | 7.02e-05 | 1.73 | 6.74e-06 | -0.65 |

Table 5.8: Numerical results (values and Greeks) for European Exchange option in spotting area using *PDE* boundary conditions. Settings in Table 5.1 and *non-uniform discretization* with mapping function (4.11) are used. The errors are calculated as infinity norms of errors of all grid points in the spotting area.

### 5.1.3 Different Localizations

As we mentioned in Chapter 3, in a numerical PDE method for a pricing problem, we usually truncate the far-sides of the two price domains to $S_{1,\infty}$ and $S_{2,\infty}$ chosen to be sufficiently large numbers compared to the spot price and spotting area. In this subsection, we want to test the effects of this far-side truncations if pay-off boundary conditions are used. The settings in Table 5.1 are used except the price domain of $S_1$ and $S_2$. In this experiment, we compare the results of domain $[0, 500] \times [0, 500]$ (Table 5.9) and domain $[0, 1000] \times [0, 1000]$ (Table 5.10) which doubles the far-side of domain of $S_1$ and $S_2$. In order to control the effect of the discretization errors in the comparison of far-side boundaries, *uniform discretization* is used. In order to have the same length of subintervals, the number of subintervals on each dimension when using domain $[0, 1000] \times [0, 1000]$ is chosen to be double the number of subintervals on each dimension when using $[0, 500] \times [0, 500]$.

From the Tables 5.9 and 5.10, we can see that both these two choices of far-side truncation give second order convergences of values of option and Greeks. When comparing these results, we find that under the same subinterval length, there are minor differences in the price and the Greeks approximations, with the differences being a little more visible for the Greeks associated with $S_2$ and when $N_1$ and $N_2$ are both small. We say that these two boundaries exhibit almost same error performance under the same subinterval length. Therefore, for the efficiency of computation, we choose to use smaller the far-side, since, under the same subinterval length, $[0, 500] \times [0, 500]$ will result in a smaller linear system.

| $N_1, N_2$ | Value ($u$) | |
|---|---|---|
| | error | order |
| 25 | 1.17e+00 | |
| 50 | 2.32e-01 | 2.33 |
| 100 | 6.12e-02 | 1.92 |
| 200 | 1.61e-02 | 1.93 |

| $N_1, N_2$ | $\Delta_{S_1}$ | | $\Gamma_{S_1}$ | | $\Delta_{S_2}$ | | $\Gamma_{S_2}$ | |
|---|---|---|---|---|---|---|---|---|
| | error | order | error | order | error | order | error | order |
| 25 | 4.97e-02 | | 2.48e-03 | | 1.31e-01 | | 1.89e-02 | |
| 50 | 1.25e-02 | 1.98 | 6.50e-04 | 1.93 | 1.61e-02 | 1.55 | 1.24e-03 | 3.93 |
| 100 | 3.57e-03 | 1.81 | 1.02e-04 | 2.67 | 5.51e-03 | 1.73 | 2.64e-04 | 2.23 |
| 200 | 1.03e-03 | 1.79 | 2.47e-05 | 1.87 | 1.67e-03 | 1.86 | 2.67e-05 | 1.53 |

Table 5.9: Numerical results (values and Greeks) for European Exchange option in spotting area using *pay-off* boundary conditions. Settings in Table 5.1 and *uniform discretization* are used. The errors are calculated as infinity norms of errors of all grid points in the spotting area.

| $N_1, N_2$ | Value ($u$) | |
|---|---|---|
| | error | order |
| 50 | 1.16e+00 | |
| 100 | 2.32e-01 | 2.33 |
| 200 | 6.11e-02 | 1.92 |
| 400 | 1.61e-02 | 1.93 |

| $N_1, N_2$ | $\Delta_{S_1}$ | | $\Gamma_{S_1}$ | | $\Delta_{S_2}$ | | $\Gamma_{S_2}$ | |
|---|---|---|---|---|---|---|---|---|
| | error | order | error | order | error | order | error | order |
| 50 | 4.97e-02 | | 2.46e-03 | | 5.00e-02 | | 3.22e-03 | |
| 100 | 1.25e-02 | 1.99 | 6.42e-04 | 1.94 | 1.61e-02 | 1.64 | 2.51e-04 | 1.86 |
| 200 | 3.46e-03 | 1.81 | 1.00e-04 | 2.68 | 5.51e-03 | 1.54 | 6.93e-04 | 1.39 |
| 400 | 1.03e-03 | 1.79 | 2.42e-05 | 2.05 | 1.67e-03 | 1.73 | 9.15e-05 | 1.52 |

Table 5.10: Numerical results (values and Greeks) for European Exchange option in spotting area using *pay-off* boundary conditions. Settings in Table 5.1 are used except the price domains of $S_1$ and $S_2$. Price domain $[0, 1000] \times [0, 1000]$ is used. *Uniform discretization* is used. The errors are calculated as infinity norms of errors of all grid points in the spotting area.

### 5.1.4 Different Parameter Settings

We also want to test sensitivity of the quality of numerical soluiton to the parameter settings. In particular, we want to test the performance under the circumstances of high volatility, high correlation and longer maturity time. Therefore, we consider the settings in Table 5.1, but change the value of parameters $T$, $\sigma_1$ and $\rho$. In this way, we produce three new sets of parameter values as shown in Table 5.11. More specifically, setting 1 has larger maturity time, setting 2 has larger $\sigma_1$ and setting 3 has larger $\rho$. In this subsection, we use the non-uniform mapping (4.11) with $\eta = 80$ and Margrabe boundary conditions.

Table 5.12 shows the numerical results corresponding to a change to a maturity time. Recall that the time-step size is $\frac{2}{N_1}$, therefore, the number of time-steps in Table 5.12 is about double compared to corresponding cases of Table 5.3. From the numerical solution of price and Greeks, we see that our numerical method exhibits slightly smaller errors for the values, Deltas and Gammas when $T$ is larger. Overall, the errors are converging at rate of approximately 2.

Table 5.13 shows the numerical results corresponding to a change in the volatility value $\sigma_1$ and should be compared to the results of Table 5.3. From the numerical solution of price and Greeks, we see that our numerical method exhibits slightly smaller error for the value and Deltas when $\sigma_1$ is larger, while slightly larger errors for the Gammas. We also notice that the Gammas are more sensitive to the volatility value. Overall, the errors are converging at rate of approximately 2.

Table 5.14 and Figure 5.1b shows the numerical results corresponding to the change in the value of coorrelation and should be compared to5.3. From the numerical solution of price and Greeks, we see that, when $\rho$ is large, our numerical method exhibits slightly smaller error for the values, while slightly larger errors for all Greeks. We also note for the Greeks, especially the Gammas, it takes a larger $N_1$ to reach the asymptotic order of convergence. We also notice that the Gamma error is more sensitive size of $\rho$ than the price of Delta errors. Overall, asymptotically, the errors are converging at rate of approximately 2.

| Parameters | value set 1 | value set 2 | value set 3 |
|---|---|---|---|
| Domain of $S_1$ | $[0, 500]$ | $[0, 500]$ | $[0, 500]$ |
| Domain of $S_2$ | $[0, 500]$ | $[0, 500]$ | $[0, 500]$ |
| Spot price | $S_1 = S_2 = 60$ | $S_1 = S_2 = 60$ | $S_1 = S_2 = 60$ |
| Spotting area | $[30, 180] \times [30, 180]$ | $[30, 180] \times [30, 180]$ | $[30, 180] \times [30, 180]$ |
| Time to maturity $T$ | **2** | 1 | 1 |
| Volatility of first asset $\sigma_1$ | 0.4 | **0.8** | 0.4 |
| Volatility of second asset $\sigma_2$ | 0.2 | 0.2 | 0.2 |
| Interest rate $r$ | 0.1 | 0.1 | 0.1 |
| Correlation $\rho$ | 0.4 | 0.4 | **0.6** |

Table 5.11: Different model parameters for pricing European Exchange option. Changes from Table 5.1 are shown in bold face.

| $N_1, N_2$ | Value $(u)$ | |
|---|---|---|
| | error | order |
| 25 | 8.32e-01 | |
| 50 | 2.13e-01 | 1.97 |
| 100 | 5.45e-02 | 1.97 |
| 200 | 1.36e-02 | 2.00 |
| 400 | 3.37e-03 | 2.01 |

| $N_1, N_2$ | $\Delta_{S_1}$ | | $\Gamma_{S_1}$ | | $\Delta_{S_2}$ | | $\Gamma_{S_2}$ | |
|---|---|---|---|---|---|---|---|---|
| | error | order | error | order | error | order | error | order |
| 25 | 1.10e-02 | | 2.61e-04 | | 1.12e-02 | | 2.68e-04 | |
| 50 | 2.74e-03 | 2.01 | 6.55e-05 | 1.99 | 2.80e-03 | 2.00 | 6.78e-04 | 1.98 |
| 100 | 6.89e-04 | 1.99 | 1.74e-05 | 1.91 | 7.07e-04 | 1.99 | 1.76e-05 | 1.85 |
| 200 | 1.73e-04 | 1.99 | 4.50e-06 | 1.95 | 1.78e-04 | 1.99 | 4.52e-06 | 1.96 |
| 400 | 4.33e-05 | 2.00 | 1.14e-06 | 1.98 | 4.45e-05 | 2.00 | 1.19e-06 | 1.92 |

Table 5.12: Numerical results (values and Greeks) for European Exchange option in spotting area using *Margrabe* boundary conditions. Value set 1 in Table 5.11 and *non-uniform discretization* with mapping function (4.11) are used. This option has longer maturity time $T = 2$. The errors are calculated as infinity norms of errors of all grid points in the spotting area.

| $N_1, N_2$ | Value ($u$) | |
|---|---|---|
| | error | order |
| 25 | 6.41e-01 | |
| 50 | 1.62e-01 | 1.99 |
| 100 | 4.19e-02 | 1.95 |
| 200 | 1.05e-02 | 2.00 |
| 400 | 2.62e-03 | 2.00 |

| $N_1, N_2$ | $\Delta_{S_1}$ | | $\Gamma_{S_1}$ | | $\Delta_{S_2}$ | | $\Gamma_{S_2}$ | |
|---|---|---|---|---|---|---|---|---|
| | error | order | error | order | error | order | error | order |
| 25 | 8.64e-03 | | 1.78e-04 | | 8.67e-03 | | 1.77e-04 | |
| 50 | 2.18e-03 | 1.98 | 4.94e-05 | 1.83 | 2.19e-03 | 1.98 | 4.90e-04 | 1.85 |
| 100 | 5.50e-04 | 1.99 | 1.31e-05 | 1.92 | 5.53e-04 | 1.92 | 1.30e-05 | 1.92 |
| 200 | 1.38e-04 | 1.99 | 3.36e-06 | 1.96 | 1.39e-04 | 1.96 | 3.33e-06 | 1.96 |
| 400 | 3.46e-05 | 2.00 | 8.53e-06 | 1.98 | 3.49e-05 | 1.98 | 8.45e-06 | 1.98 |

Table 5.13: Numerical results (values and Greeks) for European Exchange option in spotting area using *Margrabe* boundary conditions. Value set 2 in Table 5.11 and *non-uniform discretization* with mapping function (4.11) are used. First asset has high volatility $\sigma_1 = 0.8$. The errors are calculated as infinity norms of errors of all grid points in the spotting area.

| $N_1, N_2$ | Value ($u$) | |
|---|---|---|
| | error | order |
| 25 | 7.15e-01 | |
| 50 | 1.62e-01 | 2.14 |
| 100 | 4.08e-02 | 1.99 |
| 200 | 1.01e-02 | 2.01 |
| 400 | 2.52e-03 | 2.00 |

| $N_1, N_2$ | $\Delta_{S_1}$ | | $\Gamma_{S_1}$ | | $\Delta_{S_2}$ | | $\Gamma_{S_2}$ | |
|---|---|---|---|---|---|---|---|---|
| | error | order | error | order | error | order | error | order |
| 25 | 1.92e-02 | | 8.45e-04 | | 1.96e-02 | | 8.21e-04 | |
| 50 | 5.72e-03 | 1.75 | 4.47e-04 | 0.92 | 5.84e-03 | 1.75 | 4.32e-04 | 0.93 |
| 100 | 1.54e-03 | 1.89 | 1.44e-04 | 1.63 | 1.59e-03 | 1.88 | 1.42e-04 | 1.61 |
| 200 | 3.95e-04 | 1.96 | 3.95e-05 | 1.87 | 4.08e-04 | 1.96 | 3.90e-05 | 1.86 |
| 400 | 9.99e-05 | 1.99 | 1.02e-05 | 1.95 | 1.03e-04 | 1.98 | 1.01e-05 | 1.95 |

Table 5.14: Numerical results (values and Greeks) for European Exchange option in spotting area using *Margrabe* boundary conditions. Value set 3 in Table 5.11 and *non-uniform discretization* with mapping function (4.11) are used. The two assets have high correlation $\rho = 0.6$. The errors are calculated as infinity norms of errors of all grid points in the spotting area.

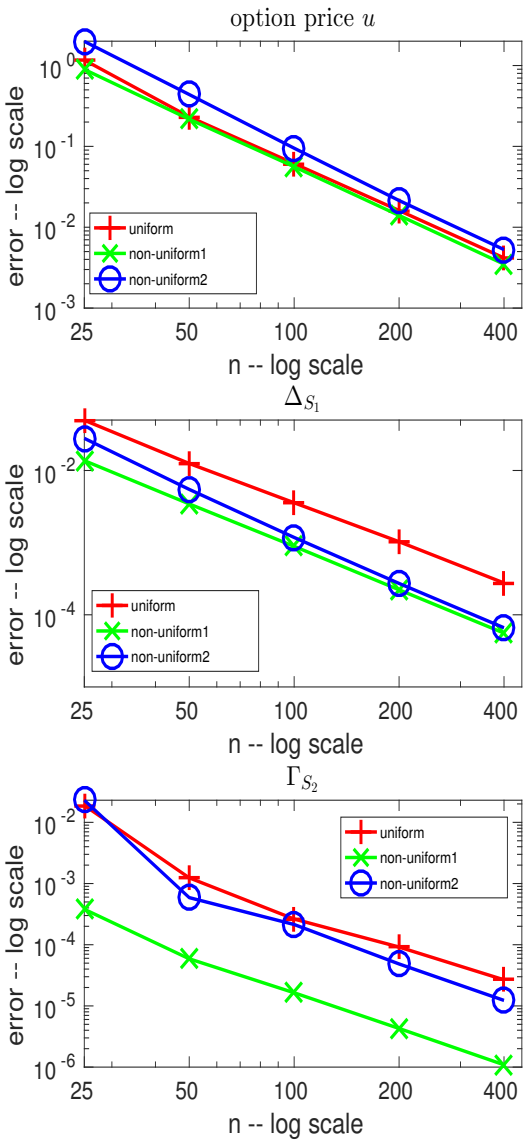


(a) Convergence study of Exchange option price, $\Delta_{S_1}$ and $\Gamma_{S_2}$ with three different space discretizations: uniform and non-uniform generated by mappings (4.11) and (4.12). Parameter settings in Table 5.1 and Margrabe boundary conditions are used.

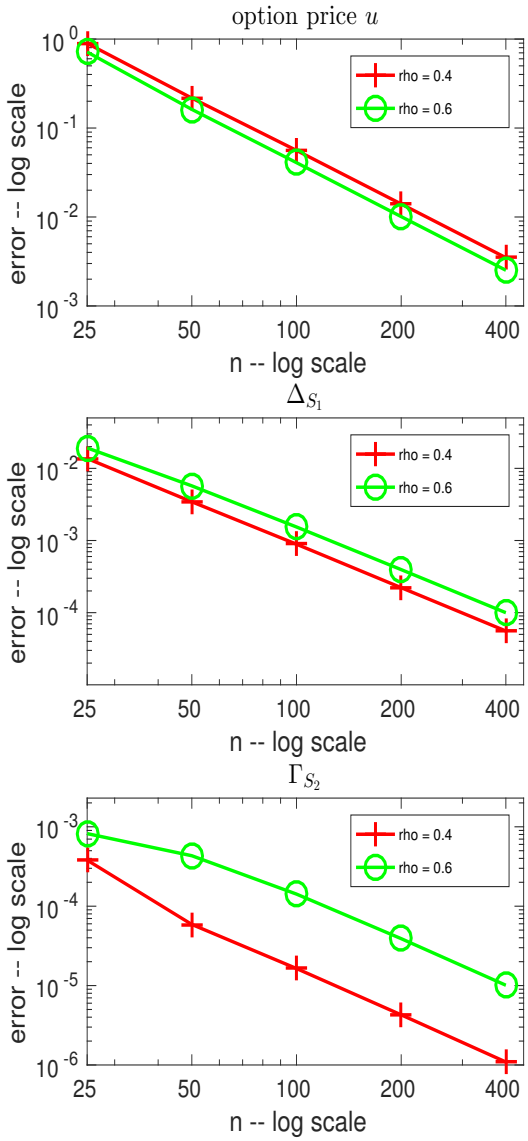


(b) Convergence study of Exchange option price, $\Delta_{S_1}$ and $\Gamma_{S_2}$ with two different correlations $\rho = 0.4$ and $\rho = 0.6$. Parameter settings in Table 5.1 (except the correlation $\rho$), non-uniform space discretization generated by (4.11) and Margrabe boundary conditions are used.

Figure 5.1: European Exchange option convergence study.

## 5.2 European Spread Option

In this section, European Spread Call options with parameter settings in Table 5.15 are priced. Recall that the pay-off of Spread Call option is defined by

$$\max(S_1 - S_2 - K, 0).$$

For European Spread options, there is no analytical formula. Therefore we approximate the convergence rates using the changes of prices with three different grid refinements as in (5.4). The order of convergence of the Greeks in the spotting area is calculated similarly as well. At the same time, some closed-form approximations for the price of European Spread option will be calculated for comparison to our numerical solutions.

| Parameters | Value |
|---|---|
| Domain of $S_1$ | $[0, 880]$ |
| Domain of $S_2$ | $[0, 480]$ |
| Strike price $K$ | 50 |
| Spot price | $S_1 = 110, S_2 = 60$ |
| Spotting area | $[88, 132] \times [48, 72]$ |
| Time to maturity $T$ | 182/365 |
| Volatility of first asset $\sigma_1$ | 0.4 |
| Volatility of second asset $\sigma_2$ | 0.2 |
| Interest rate $r$ | 0.1 |
| Correlation $\rho$ | 0.4 |

Table 5.15: Model parameters for pricing European Spread Call option

From Section 6.1, it is obvious that non-uniform space discretizations can result in more accurate solutions than uniform ones. However, as discussed before, the non-uniform discretization from mapping (4.11) may not be as effective in the Spread option case as in the Exchange option case. Therefore, experiments are conducted to test the performance of the two proposed non-uniform mappings in the Spread option case.

Regarding the far-side boundaries (i.e. when $S_1 = 660$ or $S_2 = 360$), we apply time-discounted pay-off boundary conditions, because, as seen in the previous subsection of Exchange option case, time-discounted pay-off boundary conditions give rise to acceptable values and Greeks. When $S_1 = 0$, the pay-off function suggests the Dirichlet condition $u(\tau, 0, S_2) = 0$. When $S_2 = 0$, we take the Dirichlet condition $u(\tau, S_1, 0) = \max\{S_1 - Ke^{-rt}, 0\}$.

### 5.2.1 Different Space Discretizations

Tables 5.16, 5.17 and Figure 5.2a show the results of valuing a European Spread option with two non-uniform space discretizations in our spotting area. Note that in the experiments, some points that are grid points in the refined grid discretizations are not grid points in the coarser grid discretizations. Therefore, to calculate values on these points in the coarser grid discretizations, we use spline interpolation as implemented in **MATLAB**'s function **interp2**.

From Table 5.15, we can see that the range of second asset $S_2$ is a little more than half the range of first asset $S_1$, hence we consider to set smaller number of discretization points on the axis of $S_2$, i.e. we can set $N_2$ a little more than half $N_1$. In this experiment, by testing several values of $N_2$ between $0.5N_1$ and $0.7N_1$, we found that, in the case of non-uniform mapping (4.12), the choice $N_2 \approx 0.65N_1$ is sa good choice.

From Tables 5.16 and 5.17, we find that the non-uniform discretizations generated from non-uniform mappings (4.11) and (4.12) both give stable convergence rate around 2 on the option value in the spotting area. We notice a slightly lower order of convergence, especially for the Greeks associated the Gamma ($\Gamma$), when using the non-uniform mapping (4.12) and when $N_1$ is small.

| $N_1$ | $N_2$ | value ($u$) | |
|---|---|---|---|
| | | change | order |
| 25 | 17 | | |
| 50 | 33 | 2.8762e-01 | |
| 100 | 65 | 5.5738e-02 | 2.32 |
| 200 | 130 | 1.4833e-02 | 1.96 |
| 400 | 260 | 3.9961e-03 | 1.89 |

| $N_1$ | $\Delta_{S_1}$ | | $\Gamma_{S_1}$ | | $\Delta_{S_2}$ | | $\Gamma_{S_2}$ | |
|---|---|---|---|---|---|---|---|---|
| | change | order | change | order | change | order | change | order |
| 25 | | | | | | | | |
| 50 | 1.92e-02 | | 5.38e-04 | | 5.59e-03 | | 2.11e-03 | |
| 100 | 4.66e-03 | 2.05 | 1.47e-04 | 1.87 | 1.54e-03 | 1.86 | 4.51e-04 | 2.23 |
| 200 | 1.17e-03 | 1.99 | 3.68e-05 | 2.00 | 3.55e-04 | 2.12 | 4.36e-05 | 3.37 |
| 400 | 2.86e-04 | 2.03 | 9.32e-06 | 1.98 | 9.77e-05 | 1.86 | 1.23e-05 | 1.82 |

Table 5.16: Numerical results (values and Greeks) for European Spread Call option in spotting area using pay-off boundary conditions. Settings in Table 5.15 and *non-uniform discretization* with mapping function (4.11) are used. In (4.11), parameter $\eta = 80$ for $S_2$ and $S_1$.

| $N_1$ | $N_2$ | value ($u$) | |
|---|---|---|---|
| | | change | order |
| 25 | 17 | | |
| 50 | 33 | 2.3919e-01 | |
| 100 | 65 | 4.9978e-02 | 2.26 |
| 200 | 130 | 1.3825e-02 | 1.85 |
| 400 | 260 | 3.5253e-03 | 1.97 |

| $N_1$ | $\Delta_{S_1}$ | | $\Gamma_{S_1}$ | | $\Delta_{S_2}$ | | $\Gamma_{S_2}$ | |
|---|---|---|---|---|---|---|---|---|
| | change | order | change | order | change | order | change | order |
| 25 | | | | | | | | |
| 50 | 2.65e-02 | | 9.59e-04 | | 1.29e-02 | | 4.76e-04 | |
| 100 | 2.47e-03 | 3.42 | 1.45e-04 | 2.72 | 3.90e-03 | 1.72 | 1.52e-04 | 1.65 |
| 200 | 6.24e-04 | 1.98 | 3.53e-05 | 2.04 | 1.09e-03 | 1.85 | 4.18e-05 | 1.86 |
| 400 | 1.62e-04 | 1.95 | 9.27e-06 | 1.93 | 2.69e-04 | 2.02 | 1.10e-05 | 1.93 |

Table 5.17: Numerical results (values and Greeks) for European Spread Call option in spotting area using pay-off boundary conditions. Settings in Table 5.15 and *non-uniform discretization* with mapping function (4.12) are used. In (4.12), parameter $\alpha = 0.4$ and $E = 60$ for $S_2$-axis and parameter $\alpha = 0.4$ and $E = 110$ for $S_1$-axis.

We also want to compare the performance of these two non-uniform mappings at a particular point. Here we use spot price $(110, 60)$ as an example point. From Table 5.18, the value and Delta associated with $S_1$ ($\Delta_{S_1}$) on the spotting area converge monotonically with straight order 2. However, we find on this point, the values of other Greeks associated with $S_2$ fail to converge monotonically.

At the same time, from Table 5.19, the convergence rate of values and Greeks on this point appears more stable around 2. It seems that, because the second non-uniform mapping (4.12) can push more grid points towards the point of interest, this mapping helps to achieve more stable performance at that point.

To conclude, each of these two different non-uniform discretizations has its own advantages. The first non-uniform mapping (4.11) results in the convergence with straight order 2 in the spotting area. However, it may fail to ensure the second order convergence of Greeks at some specific points in the spotting area. Meanwhile the second non-uniform mapping (4.12) results in the second order convergence of option prices and Greeks at a particular point if that point is chosen as concentration point. Overall, looking at Figures 5.2a and 5.2b, the performance of mapping (4.12) is better and more stable regardless of option values or Greeks. In addition to the asymptotic performance of the two different mappings, the second mapping (4.12) also maintains a stable result with smaller space

discretization. Therefore, we conclude that the second mapping (4.12) is a better choice in the case of Spread option.

| $N_1$ | Option price | | |
|---|---|---|---|
| | Value | Change | Order |
| 25 | 12.290238 | | |
| 50 | 12.493087 | 2.03e-01 | |
| 100 | 12.541964 | 4.89e-02 | 2.05 |
| 200 | 12.553647 | 1.17e-02 | 2.06 |
| 400 | 12.557227 | 3.58e-03 | 1.71 |

| $N_1$ | $\Delta_{S_1}$ | | | $\Gamma_{S_1}$ | | |
|---|---|---|---|---|---|---|
| | Value | Change | Order | Value | Change | Order |
| 25 | 0.5622557 | | | 0.01354978 | | |
| 50 | 0.5799406 | 1.77e-02 | | 0.01356923 | 1.95e-05 | |
| 100 | 0.5842087 | 4.27e-03 | 2.05 | 0.01356707 | -2.16e-06 | 3.17 |
| 200 | 0.5852799 | 1.07e-03 | 1.99 | 0.01356761 | -5.36e-07 | 2.01 |
| 400 | 0.5855516 | 2.72e-04 | 1.98 | 0.01356694 | -6.67e-07 | -0.32 |

| $N_1$ | $\Delta_{S_2}$ | | | $\Gamma_{S_2}$ | | |
|---|---|---|---|---|---|---|
| | Value | Change | Order | Value | Change | Order |
| 25 | -0.4847673 | | | 0.01438115 | | |
| 50 | -0.4845619 | 2.05e-04 | | 0.01439833 | 1.72e-05 | |
| 100 | -0.4854671 | -9.05e-04 | -2.14 | 0.01428701 | -1.11e-04 | -2.70 |
| 200 | -0.4853534 | 1.14e-04 | 2.99 | 0.01426288 | -2.41e-05 | 2.21 |
| 400 | -0.4853922 | 3.88e-05 | 1.55 | 0.01425878 | -4.10e-06 | 2.56 |

Table 5.18: Numerical results (values and Greeks) of European Spread Call option when $S_1 = 110, S_2 = 60$ using pay-off boundary conditions. Settings in Table 5.15 and *non-uniform discretization* with mapping function (4.11) are used. In (4.11), parameter $\eta = 80$ for $S_1$ and $S_2$.

| $N_1$ | Option price | | |
|---|---|---|---|
| | Value | Change | Order |
| 25 | 12.401970 | | |
| 50 | 12.518983 | 1.17e-01 | |
| 100 | 12.548484 | 2.95e-02 | 1.99 |
| 200 | 12.555880 | 7.40e-03 | 2.00 |
| 400 | 12.557728 | 1.85e-03 | 2.00 |

| $N_1$ | $\Delta_{S_1}$ | | | $\Gamma_{S_1}$ | | |
|---|---|---|---|---|---|---|
| | Value | Change | Order | Value | Change | Order |
| 25 | 0.5832525 | | | 0.01345684 | | |
| 50 | 0.5850403 | 1.79e-03 | | 0.01353910 | 8.23e-05 | |
| 100 | 0.5854919 | 4.52e-04 | 1.99 | 0.01355995 | 2.08e-05 | 1.98 |
| 200 | 0.5856041 | 1.12e-04 | 2.01 | 0.01356509 | 5.14e-06 | 2.02 |
| 400 | 0.5856322 | 2.82e-05 | 1.99 | 0.01356638 | 1.29e-06 | 2.00 |

| $N_1$ | $\Delta_{S_2}$ | | | $\Gamma_{S_2}$ | | |
|---|---|---|---|---|---|---|
| | Value | Change | Order | Value | Change | Order |
| 25 | -0.4890363 | | | 0.01462652 | | |
| 50 | -0.4862420 | 2.79e-03 | | 0.01436166 | -2.65e-04 | |
| 100 | -0.4856252 | 6.17e-04 | 2.18 | 0.01428049 | -8.12e-05 | 1.71 |
| 200 | -0.4854496 | 1.76e-04 | 1.81 | 0.01426294 | -1.76e-05 | 2.21 |
| 400 | -0.4854085 | 4.11e-05 | 2.10 | 0.01425779 | -5.15e-06 | 1.77 |

Table 5.19: Numerical results (values and Greeks) of European Spread Call option when $S_1 = 110, S_2 = 60$ using pay-off boundary conditions. Settings in Table 5.15 and *non-uniform discretization* with mapping function (4.12) are used. In (4.12), parameter $\alpha = 0.36$ and $E = 60$ for $S_2$-axis and parameter $\alpha = 0.4$ and $E = 110$ for $S_1$-axis.

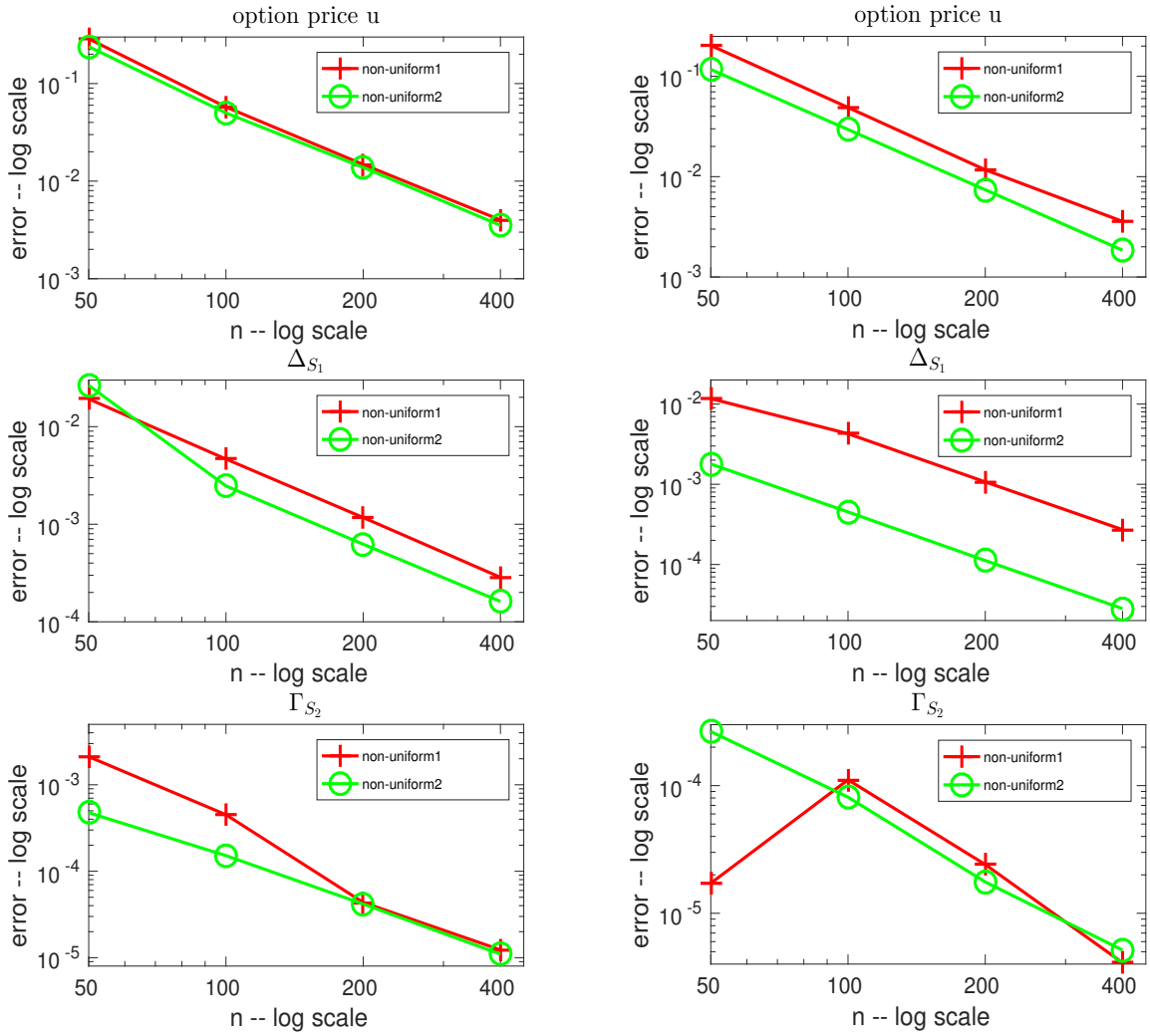


(a) Convergence study of numerical results of option solution, $\Delta_{S_1}$ and $\Gamma_{S_2}$ in spotting area with two different space discretizations: non-uniform generated by mappings (4.11) and (4.12). Parameter settings in Table 5.15 and pay-off boundary conditions are used.

(b) Convergence study of numerical results of option solution, $\Delta_{S_1}$ and $\Gamma_{S_2}$ on point (110, 60) with two different space discretizations: non-uniform generated by mappings (4.11) and (4.12). Parameter settings in Table 5.15 and pay-off boundary conditions are used.

Figure 5.2: European Spread Call option convergence study.

### 5.2.2 Comparison to Analytical Approximations

To compare our numerical methods with analytical approximations, we consider the numerical PDE approximations from Table 5.19 and compare them with closed-form approximations mentioned in Chapter 3. Table 5.20 shows the results.

When comparing numerical PDE and analytical approximations, we notice the following advantages and disadvantages of each. The numerical PDE error converges to zero as the grid discretization is refined, which means that when enough computational power is used, the error goes below a given tolerance. At the same time, the errors of analytical approximations remain constant. However, analytical approximations require less computation work compared to numerical PDE methods. It seems that for the particular Spread option being priced, Kirk's approximation is about accurate as when $N_1 = 400, N_2 = 260$ while Deng, Li and Zhou's Approximation is at least as accurate as $N_1 = 800, N_2 = 520$ PDE approximation.

From Figure 5.3, we can easily observe that the numerical solution on point (110, 60) is converging to a number, which is greater than Kirk's approximation (12.5574715) but closer to Deng, Li and Zhou's approximation (12.5583468). From this point of view, we conclude that Deng, Li and Zhou's approximation is a more accurate analytical solution than Kirk's approximation.

Moreover, we note that the difference of numerical PDE and Deng, Li and Zhou's approximations converges at order 2 even up to $N_1 = 800, N_2 = 520$. This suggests that the accuracy of Deng, Li and Zhou's approximation is possibly higher than the numerical PDE solution with $N_1 = 800, N_2 = 520$. However, we also note that Deng, Li and Zhou's approximation holds for European and not for American Spread options, while the numerical PDE approach can be extended to American.

| Kirk's Approximation [12] | 12.5574715 |
|---|---|
| Deng, Li and Zhou's Approximation [13] | 12.5583468 |

| $N_1$ | Option price | | | NPDE - KirK | NPDE - DLZ |
|---|---|---|---|---|---|
| | Value | Change | Order | | |
| 25 | 12.401970 | | | -0.1555013 | -0.1563766 |
| 50 | 12.518983 | 1.17e-01 | | -0.0384884 | -0.0393637 |
| 100 | 12.548484 | 2.95e-02 | 1.99 | -0.0089876 | -0.0098629 |
| 200 | 12.555880 | 7.40e-03 | 2.00 | -0.0015915 | -0.0024668 |
| 400 | 12.557728 | 1.85e-03 | 2.00 | 0.0002562 | -0.0006191 |
| 800 | 12.558190 | 4.62e-04 | 2.00 | 0.0007185 | -0.0001568 |

Table 5.20: Numerical and analytical approximations to the value of European Spread Call option when $S_1 = 110, S_2 = 60$. NPDE - KirK means the difference between numerical PDE and Kirk's approximations. NPDE - DLZ means the difference between numerical PDE and Deng, Li and Zhou's approximations.

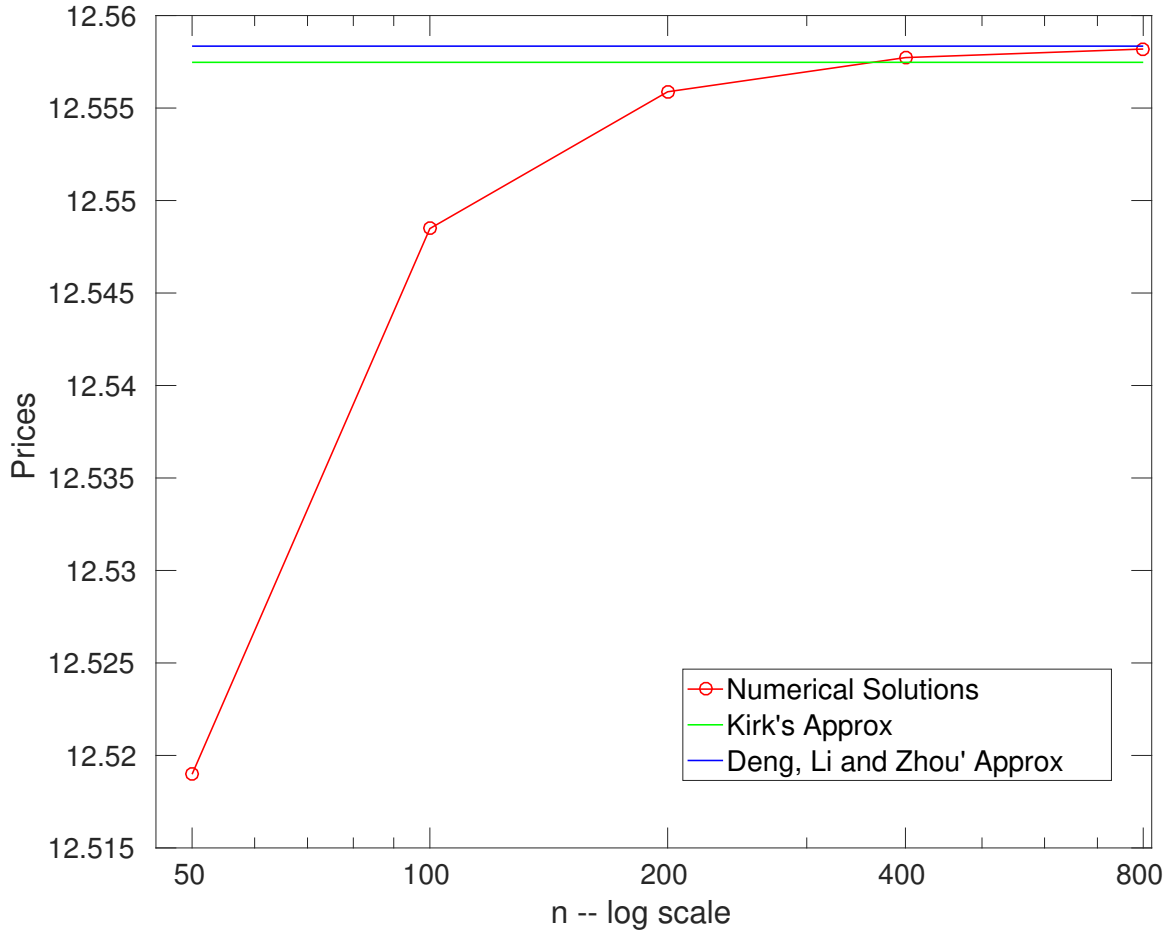


Figure 5.3: Plot of numerical PDE and analytical approximations to the value of European Spread Call option when $S_1 = 110, S_2 = 60$ versus grid size.

### 5.2.3 European Spread Put option

Beside the experiments of European Spread Call option, the case of European Spread Put option is also shown below. These results can be used for comparison to the American type option shown in the next section. Recall that the pay-off of European Spread Put option is defined as

$$\max(S_2 + K - S_1, 0).$$

The parameter settings in Table 5.15 are considered. In this experiment, we set $N_2 \approx 0.65N_1$, since this choice of $N_1$ and $N_2$ is successful in the case of European Spread call options. We also use the second non-uniform mapping (4.12). It is interesting to

observe from Tables 5.19 and 5.22 that, the errors of Spread call option and Spread put option with exactly the same settings are almost the same for prices and Greeks. The approximation to the Gammas ($\Gamma$) of Spread call and put options are also almost the same with same grid discretizations.

| $N_1$ | $N_2$ | value ($u$) | |
|---|---|---|---|
| | | change | order |
| 25 | 17 | | |
| 50 | 33 | 6.0665e-01 | |
| 100 | 65 | 5.6665e-02 | 3.42 |
| 200 | 130 | 1.3808e-02 | 2.04 |
| 400 | 260 | 3.5209e-03 | 1.97 |

| $N_1$ | $\Delta_{S_1}$ | | $\Gamma_{S_1}$ | | $\Delta_{S_2}$ | | $\Gamma_{S_2}$ | |
|---|---|---|---|---|---|---|---|---|
| | change | order | change | order | change | order | change | order |
| 25 | | | | | | | | |
| 50 | 7.95e-02 | | 8.16e-03 | | 1.29e-02 | | 4.76e-04 | |
| 100 | 2.47e-03 | 5.01 | 3.30e-04 | 4.63 | 3.90e-03 | 1.72 | 1.52e-04 | 1.65 |
| 200 | 6.24e-04 | 1.98 | 3.53e-05 | 3.22 | 1.09e-03 | 1.85 | 4.18e-05 | 1.86 |
| 400 | 1.62e-04 | 1.95 | 9.27e-06 | 1.93 | 2.69e-04 | 2.02 | 1.10e-05 | 1.93 |

Table 5.21: Numerical results (values and Greeks) for European Spread put option in spotting area using pay-off boundary conditions. Settings in Table 5.15 and *non-uniform discretization* with mapping function (4.12) are used. In (4.12), parameter $\alpha = 0.4$ and $E = 110$ for $S_1$-axis and parameter $\alpha = 0.4$ and $E = 60$ for $S_2$-axis.

| $N_1$ | Option price | | |
|---|---|---|---|
| | Value | Change | Order |
| 25 | 9.970339 | | |
| 50 | 10.087064 | 1.17e-01 | |
| 100 | 10.116494 | 2.94e-02 | 1.99 |
| 200 | 10.123873 | 7.38e-03 | 2.00 |
| 400 | 10.125716 | 1.84e-03 | 2.00 |

| $N_1$ | $\Delta_{S_1}$ | | | $\Gamma_{S_1}$ | | |
|---|---|---|---|---|---|---|
| | Value | Change | Order | Value | Change | Order |
| 25 | 0.4167478 | | | 0.01345686 | | |
| 50 | 0.4149597 | 1.79e-03 | | 0.01353910 | 8.22e-05 | |
| 100 | 0.4145081 | 4.52e-04 | 1.99 | 0.01355995 | 2.08e-05 | 1.98 |
| 200 | 0.4143959 | 1.12e-04 | 2.01 | 0.01356509 | 5.14e-06 | 2.02 |
| 400 | 0.4143678 | 2.82e-05 | 1.99 | 0.01356638 | 1.29e-06 | 2.00 |

| $N_1$ | $\Delta_{S_2}$ | | | $\Gamma_{S_2}$ | | |
|---|---|---|---|---|---|---|
| | Value | Change | Order | Value | Change | Order |
| 25 | -0.5109623 | | | 0.01462688 | | |
| 50 | -0.5137580 | 2.80e-03 | | 0.01436166 | -2.65e-04 | |
| 100 | -0.5143748 | 6.17e-04 | 2.18 | 0.01428049 | -8.12e-05 | 1.71 |
| 200 | -0.5145504 | 1.76e-04 | 1.81 | 0.01426294 | -1.76e-05 | 2.21 |
| 400 | -0.5145915 | 4.11e-05 | 2.10 | 0.01425779 | -5.15e-06 | 1.77 |

Table 5.22: Numerical results (values and Greeks) of European Spread put option when $S_1 = 110, S_2 = 60$ using pay-off boundary conditions. Settings in Table 5.15 and *non-uniform discretization* with mapping function (4.12) are used. In (4.12), parameter $\alpha = 0.4$ and $E = 110$ for $S_1$-axis and parameter $\alpha = 0.4$ and $E = 110$ for $S_2$-axis.

## 5.3 American Spread Put option

In this section, American Spread Put option with parameter setting in Table 5.23 is considered. Recall that the pay-off of American Spread Put option is defined as

$$\max(S_2 + K - S_1, 0).$$

The additional constraints of American option is that the option price can never go below the pay-off.

For American Spread options, an analytical formula for the solution is not available. Therefore we approximate convergence rates using the changes of different grid refine-

ments in (5.4). The order of convergence of the Greeks in the spotting area is calculated similarly.

In this experiment, we set $N_2 \approx 0.65N_1$ since this choice of $N_1$ and $N_2$ is successful in the case of European Spread call options. We also use the second non-uniform mapping (4.12). In the penalty method for the American options, we choose the penalty factor $p = 10^6$, while the tolerance for penalty iteration is $\frac{1}{p}$. We denote by $N_t$ the total number of timesteps, and by "p. it" the total number of iterations required in the penalty methods over all timesteps.

| Parameters | Value |
|---|---|
| Domain of $S_1$ | $[0, 880]$ |
| Domain of $S_2$ | $[0, 480]$ |
| Strike price $K$ | 50 |
| Spot price | $S_1 = 110, S_2 = 60$ |
| Spotting area | $[88, 132] \times [48, 72]$ |
| Time to maturity $T$ | 182/365 |
| Volatility of first asset $\sigma_1$ | 0.4 |
| Volatility of second asset $\sigma_2$ | 0.2 |
| Interest rate $r$ | 0.1 |
| Correlation $\rho$ | 0.4 or 0.6 |

Table 5.23: Model parameters for pricing American Spread Put option

| $N_1$ | $N_2$ | $N_t$ | p. it | value ($u$) | |
|---|---|---|---|---|---|
| | | | | change | order |
| 25 | 17 | 27 | 70 | | |
| 50 | 33 | 52 | 153 | 2.0582e-01 | |
| 100 | 65 | 102 | 273 | 3.3235e-02 | 2.63 |
| 200 | 130 | 202 | 500 | 8.9081e-03 | 1.90 |
| 400 | 260 | 401 | 924 | 2.4002e-03 | 1.89 |

| $N_1$ | $\Delta_{S_1}$ | | $\Gamma_{S_1}$ | | $\Delta_{S_2}$ | | $\Gamma_{S_2}$ | |
|---|---|---|---|---|---|---|---|---|
| | change | order | change | order | change | order | change | order |
| 25 | | | | | | | | |
| 50 | 5.19e-03 | | 6.03e-04 | | 6.25e-03 | | 1.46e-03 | |
| 100 | 9.05e-04 | 2.52 | 1.04e-04 | 2.54 | 1.18e-03 | 2.40 | 4.11e-04 | 1.82 |
| 200 | 2.41e-04 | 1.91 | 2.21e-05 | 2.23 | 2.99e-04 | 1.98 | 9.36e-05 | 2.14 |
| 400 | 6.00e-05 | 2.01 | 1.34e-06 | 4.04 | 7.26e-05 | 2.04 | 1.04e-05 | 3.17 |

Table 5.24: Numerical results (values and Greeks) for American Spread Put option in spotting area using pay-off boundary conditions. Settings in Table 5.23 with $\rho = 0.4$ and *non-uniform discretization* with mapping function (4.12) are used. In (4.12), parameter $\alpha \approx 0.38$ and $E = 110$ for $S_1$-axis and parameter $\alpha \approx 0.38$ and $E = 60$ for $S_2$-axis.

Tables 5.24 and 5.25 present our numerical results for an American Spread Put option when $\rho = 0.4$. Our FDM with penalty iteration method reaches second order or greater than second order of convergence in spotting area which is $\pm 20\%\cdot$(spot price) away from spot price. On the spot price $(110, 60)$, the order of convergence is also straight 2 for the option price and Greeks.

Looking at the total number of penalty iterations in Table 5.24, we can easily find that the average number of penalty iterations in each timestep is between 2.31 and 3.06, and for the finest grids, it is 2.31. The average number of penalty iterations indicates that the convergence of penalty iteration is independent of the discretization size. Overall, in each timestep, the penalty iteration will converge in around 2 or 3 iterations, and asymptotically, as the discretization is refined, in a number of iterations closer to 2.

| $N_1$ | $N_2$ | $N_t$ | p. it | Option price | | |
|---|---|---|---|---|---|---|
| | | | | Value | Change | Order |
| 25 | 17 | 27 | 70 | 10.196771 | | |
| 50 | 33 | 52 | 153 | 10.315621 | 1.19e-01 | |
| 100 | 65 | 102 | 273 | 10.336523 | 2.09e-02 | 2.51 |
| 200 | 130 | 202 | 500 | 10.342235 | 5.71e-03 | 1.87 |
| 400 | 260 | 401 | 924 | 10.343752 | 1.52e-03 | 1.91 |

| $N_1$ | $\Delta_{S_1}$ | | | $\Gamma_{S_1}$ | | |
|---|---|---|---|---|---|---|
| | Value | Change | Order | Value | Change | Order |
| 25 | -0.4299913 | | | 0.01420241 | | |
| 50 | -0.4275921 | 2.40e-03 | | 0.01426738 | 6.50e-05 | |
| 100 | -0.4271855 | 4.07e-04 | 2.56 | 0.01427948 | 1.21e-05 | 2.42 |
| 200 | -0.4270791 | 1.06e-04 | 1.93 | 0.01428164 | 2.16e-06 | 2.49 |
| 400 | -0.4270520 | 2.71e-05 | 1.97 | 0.01428202 | 3.72e-07 | 2.54 |

| $N_1$ | $\Delta_{S_2}$ | | | $\Gamma_{S_2}$ | | |
|---|---|---|---|---|---|---|
| | Value | Change | Order | Value | Change | Order |
| 25 | 0.5235387 | | | 0.01500219 | | |
| 50 | 0.5262912 | 2.40e-03 | | 0.01477449 | -2.28e-04 | |
| 100 | 0.5266728 | 4.07e-04 | 2.85 | 0.01471075 | -6.37e-05 | 1.84 |
| 200 | 0.5267620 | 1.06e-04 | 2.10 | 0.01469213 | -1.86e-05 | 1.78 |
| 400 | 0.5247881 | 2.71e-05 | 1.77 | 0.01468796 | -4.17e-06 | 2.16 |

Table 5.25: Numerical results (values and Greeks) of American Spread Put option when $S_1 = 110, S_2 = 60$ using pay-off boundary conditions. Settings in Table 5.23 with $\rho = 0.4$ and *non-uniform discretization* with mapping function (4.12) are used. In (4.12), parameter $\alpha \approx 0.38$ and $E = 110$ for $S_1$-axis and parameter $\alpha \approx 0.38$ and $E = 60$ for $S_2$-axis.

We are also interested in the performance of our numerical methods (FDM with penalty iteration) for the case of high correlation in American Spread Put option. Tables 5.26 and 5.27 present our numerical results for an American Spread Put option when $\rho = 0.6$. The results show us that our method still achieves accurate numerical solution to the option price and Greeks. The order of convergence in the spotting area is still around two. The numerical solution and Greeks on spotting point $(110, 60)$ are also converging with almost second order. Looking at Figure 5.4b, although the performance of numerical methods is stable under both the case of normal correlation ($\rho = 0.4$) and that of high correlation ($\rho = 0.6$), the case of normal correlation exhibits slightly smaller errors than high correlation especially on the Greeks.

| $N_1$ | $N_2$ | $N_t$ | p. it | value ($u$) | |
|---|---|---|---|---|---|
| | | | | change | order |
| 25 | 17 | 27 | 75 | | |
| 50 | 33 | 52 | 155 | 2.1283e-01 | |
| 100 | 65 | 102 | 298 | 3.5204e-02 | 2.60 |
| 200 | 130 | 202 | 518 | 9.6574e-03 | 1.86 |
| 400 | 260 | 401 | 919 | 2.5465e-03 | 1.92 |

| $N_1$ | $\Delta_{S_1}$ | | $\Gamma_{S_1}$ | | $\Delta_{S_2}$ | | $\Gamma_{S_2}$ | |
|---|---|---|---|---|---|---|---|---|
| | change | order | change | order | change | order | change | order |
| 25 | | | | | | | | |
| 50 | 6.59e-03 | | 1.38e-03 | | 7.96e-03 | | 3.00e-03 | |
| 100 | 1.28e-03 | 2.37 | 2.18e-04 | 2.56 | 1.83e-03 | 2.12 | 6.87e-04 | 2.13 |
| 200 | 3.42e-04 | 1.90 | 6.87e-05 | 1.67 | 4.35e-04 | 2.08 | 1.80e-04 | 1.93 |
| 400 | 8.59e-05 | 1.99 | 1.55e-05 | 2.15 | 1.06e-04 | 2.03 | 4.83e-05 | 1.90 |

Table 5.26: Numerical results (values and Greeks) for American Spread Put option in spotting area using pay-off boundary conditions. Settings in Table 5.23 with $\rho = 0.6$ and *non-uniform discretization* with mapping function (4.12) are used. In (4.12), parameter $\alpha \approx 0.38$ and $E = 110$ for $S_1$-axis and parameter $\alpha \approx 0.38$ and $E = 60$ for $S_2$-axis.

| $N_1$ | $N_2$ | $N_t$ | p. it | Option price | | |
|---|---|---|---|---|---|---|
| | | | | Value | Change | Order |
| 25 | 17 | 27 | 75 | 9.434413 | | |
| 50 | 33 | 52 | 155 | 9.563605 | 1.29e-01 | |
| 100 | 65 | 102 | 298 | 9.585702 | 2.21e-02 | 2.55 |
| 200 | 130 | 202 | 518 | 9.591706 | 6.00e-03 | 1.88 |
| 400 | 260 | 401 | 919 | 9.593279 | 1.57e-03 | 1.93 |

| $N_1$ | $\Delta_{S_1}$ | | | $\Gamma_{S_1}$ | | |
|---|---|---|---|---|---|---|
| | Value | Change | Order | Value | Change | Order |
| 25 | -0.4326029 | | | 0.01530520 | | |
| 50 | -0.4295972 | 3.01e-03 | | 0.01537375 | 6.86e-05 | |
| 100 | -0.4290432 | 5.54e-04 | 2.44 | 0.01538542 | 1.17e-05 | 2.55 |
| 200 | -0.4288987 | 1.44e-05 | 1.94 | 0.01538736 | 1.94e-06 | 2.59 |
| 400 | -0.4288622 | 3.65e-05 | 1.99 | 0.01538767 | 3.07e-07 | 2.66 |

| $N_1$ | $\Delta_{S_2}$ | | | $\Gamma_{S_2}$ | | |
|---|---|---|---|---|---|---|
| | Value | Change | Order | Value | Change | Order |
| 25 | 0.5126573 | | | 0.01671908 | | |
| 50 | 0.5151992 | 2.54e-03 | | 0.01604661 | -6.72e-04 | |
| 100 | 0.5155060 | 3.07e-04 | 3.05 | 0.01589755 | -1.49e-04 | 2.17 |
| 200 | 0.5155849 | 7.88e-05 | 1.96 | 0.01585872 | -3.88e-05 | 1.94 |
| 400 | 0.5156091 | 2.43e-05 | 1.70 | 0.01584949 | -9.23e-06 | 2.07 |

Table 5.27: Numerical results (values and Greeks) of American Spread Put option when $S_1 = 110, S_2 = 60$ using pay-off boundary conditions. Settings in Table 5.23 with $\rho = 0.6$ and *non-uniform discretization* with mapping function (4.12) are used. In (4.12), parameter $\alpha \approx 0.38$ and $E = 110$ for $S_1$-axis and parameter $\alpha \approx 0.38$ and $E = 60$ for $S_2$-axis.

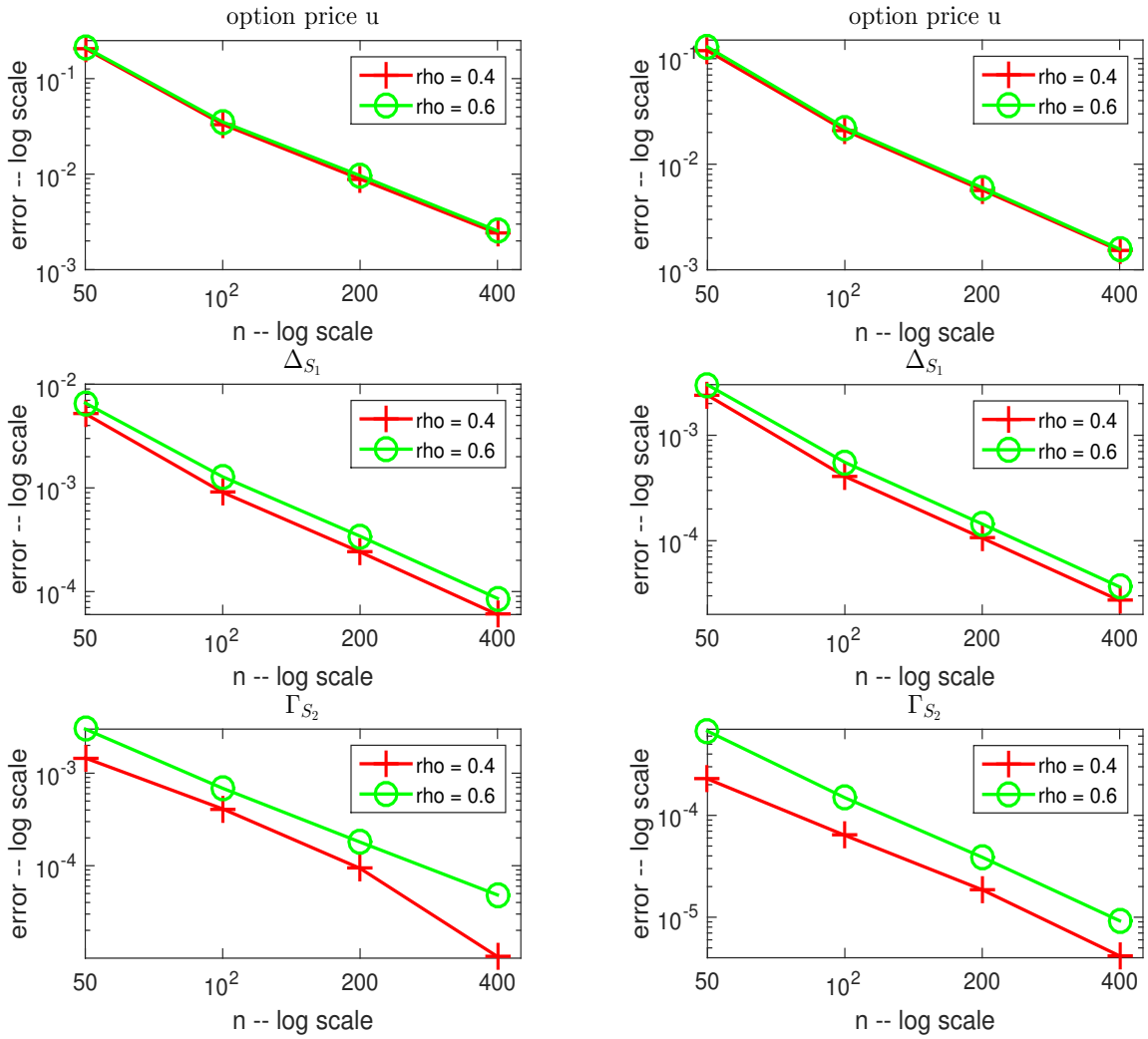


(a) Convergence study of option price, $\Delta_{S_1}$ and $\Gamma_{S_2}$ in spotting area with two different correlations: $\rho = 0.4$ and $\rho = 0.6$. Parameter settings in Table 5.23 and pay-off boundary conditions are used.

(b) Convergence study of option price, $\Delta_{S_1}$ and $\Gamma_{S_2}$ on point (110, 60) with two different correlations: $\rho = 0.4$ and $\rho = 0.6$. Parameter settings in Table 5.23 and pay-off boundary conditions are used.

Figure 5.4: American Spread Put option convergence study.

## 5.4 Iterative Method Solver for Linear System

| $N_1$ | $N_2$ | $N_t$ | value (nofill) | | | value (ilutp) | | |
|---|---|---|---|---|---|---|---|---|
| | | | error | order | tot iter | error | order | tot iter |
| 25 | 25 | 15 | 8.9665e-01 | | 32 | 8.9665e-01 | | 32 |
| 50 | 50 | 27 | 2.1676e-01 | 2.05 | 55 | 2.1676e-01 | 2.05 | 59 |
| 100 | 100 | 52 | 5.6322e-02 | 1.94 | 105 | 5.6322e-02 | 1.94 | 108 |
| 200 | 200 | 102 | 1.4214e-02 | 1.99 | 205 | 1.4214e-02 | 1.99 | 206 |
| 400 | 400 | 202 | 3.7147e-03 | 1.94 | 400 | 3.7152e-03 | 1.94 | 405 |

Table 5.28: Errors of European Exchange option. GMRES and ILU preconditioning with "nofill" (nofill) and "ilutp" (drop-tolerance) are used. The total number of iterations is denoted by "tot iter".

The test on the performance of ILU-preconditioned GMRES is conducted on the example case of the European Exchange option with parameters in Table 5.7, and uses the non-uniform mapping (4.12) and the pay-off boundary conditions. In Table 5.28, we show the performance of the two different versions of the ILU preconditioner, denoted by 'nofill' and 'ilutp' in the **MATLAB** version of GMRES. The tolerance for GMRES is set to $10^{-9}$ and the threshold parameter for the *drop-tolerance* ILU is set to $10^{-3}$.

Regarding the accuracy, both types of ILU give almost identical prices, which are also almost the same as the prices from the direct solver in Table 5.7. Only when $N_1 = N_2 = 400$, the two ILU versions have a small difference on the fourth digit of errors. As expected from theory, the second-order convergence is obtained.

In terms of total number of iterations, the two versions of ILU perform about the same. However, generally, the total number of iterations of zero fill-in ILU is slightly smaller than drop-tolerance ILU. With zero fill-in ILU, the number of iterations in each timestep is very consistent for all different discretization sizes. It is actually 3 iterations at the first timestep, and 2 iterations for every subsequent timestep. With drop-tolerance ILU, the number of iterations in each timestep fluctuates between 2 and 3 in the first few (less than 5) timesteps and then only 2 iterations are needed. Based on the performance of the total number of iterations and the consistency of convergence in each timestep, we suggest that zero fill-in ILU is preferred.

We also note that, asymptotically, for each doubling of the number of timesteps and grid points in both directions, the total number of iterations doubles approximately as well. It is also evident that the average number of iterations required by the GMRES method per timestep is quite small (around 2 iterations). More importantly, we notice

that the average number of iterations in each time step is independent of the size of discretization matrices. Since each solution with the preconditioner has computational cost proportional to the number of unknowns and the number of iterations is independent of the problem size, the total cost of the ILU preconditioned GMRES solution of the two-asset Black-Scholes PDE is proportional to the number of unknowns. Furthermore, we note that ILU is needed only once for all timesteps, since, for this PDE problem, the PDE coefficients are time independent. We also note that, because of the fast convergence of GMRES method, no restarting is needed in GMRES.

This experiment proves the efficiency of GMRES method on our problem, when using an effective preconditioner and a good initial guess based on linear extrapolation.

# Chapter 6

# Summary and Future Work

## 6.1 Summary

Multi-asset options are common in the financial market, therefore the accurate and efficient pricing of them is important. For most multi-asset European options and all American options, there is no analytical formula giving their price, therefore, numerical methods are employed to approximate the price and Greeks.

In this thesis, we choose the numerical PDE approach to value two-asset Exchange and Spread options of European or American type. We discretize the two-dimensional Black-Scholes PDE by standard centered finite differences on a rectangular grid in space and the Crank-Nicolson-Rannacher scheme in time. We study the effect of various numerical and problem parameters on the accuracy of the numerical solution value and Greeks. We also study certain numerical choices affecting the stability and the efficiency of the numerical method. For American options, we use the discrete penalty iteration method to approximate the solution of the arising LCP. In all cases, the computed price and Greeks exhibit second order convergence. Moreover, we compare the PDE approximations of European Spread option prices with those obtained by certain analytical approximation formulae found in the literature.

Regarding the type of grid discretizations, our numerical experiments indicate that non-uniform grids, with appropriate concentration of grid points, give quite more accurate prices and Greeks than uniform ones. Among the two non-uniform grids tested, the one that concentrates points towards the origin is slightly preferred for Exchange options, however, for the (more interesting) case of Spread options, the grid that concentrates points around the evaluation point seems to be superior for both values and Greeks.

Regarding the choice of boundary conditions, our numerical experiments on Exchange options indicate that Margrabe Dirichlet (exact value given) conditions are not partic-

ularly better than payoff Dirichlet or PDE boundary conditions. Furthermore, in some cases, PDE boundary conditions may give rise to smaller errors. However, it is numerically shown that PDE boundary conditions suffer from (small) instability, which may reduce the accuracy of the approximation when the number of timesteps is large. We conclude that payoff Dirichlet boundary conditions, which are applicable even if the exact value is not given on the boundary, are the conditions of choice.

Regarding the price domain localizations when using pay-off boundary conditions, our numerical experiments show that, if the far-side is sufficiently large compared to our spot price and spotting area, the truncated far-side boundary does not have an obvious effect to the errors in our spotting area. Among the two different far-side boundaries tested in the Exchange option case, the smaller price domain is preferred, because, with similar error level in price and Greeks, the smaller domain always results in smaller linear system., therefore less computation.

Regarding the effect of various problem parameters on the accuracy of the numerical solution value and Greeks, our numerical experiments indicate that (a) larger maturity time results in slightly smaller errors, when the size of the timestep is the same; (b) larger volatilities result in smaller errors, for value and Deltas and larger for Gammas; (c) larger correlation result in slightly smaller error for the value, but larger errors for the Greeks; furthermore, with a larger correlation, the asymptotic rate of convergence is reached for larger grids.

By comparing the PDE approximations of European Spread option prices with those obtained by Kirk's and Li, Deng and Zhou formulae, we find that the Li, Deng and Zhou formula is more accurate than Kirk's, and that it is at least as accurate as the numerical PDE approximation, for $[0, 880] \times [0, 480]$ spatial domain, discretized on a $800 \times 520$ grid with a 0.0025 time stepsize. This shows that the Li, Deng and Zhou formula is a competitive alternative to numerical PDE approximations. However, it should be noted that numerical PDE approximations become increasingly more accurate as the discretization size is refined, while asymptotic approximations do not possess the property. Furthermore, the asymptotic approximations do not apply to the American option case.

Regarding the American type options, our numerical results indicate that the discrete penalty iteration method converges in approximately 2-3 iterations per timestep, independently of the grid discretization, and of the correlation parameter value.

Finally, our numerical results when solving the large sparse linear system arising at each timestep by an ILU-preconditioned GMRES iterative method indicate that the number of iterations per timestep (with either zero fill-in or with a threshold parameter

controlled fill-in) is about 2, independently of the grid discretization, and, therefore, the ILU-GMRES solver has complexity proportional to the number of unknowns, making it an asymptotically optimal solver.

## 6.2 Future Work

In Chapter 5, we mentioned the ADI timestepping method as an efficient alternative to CN, which we may consider in the future. This timestepping method uses the idea of operator splitting to solve parabolic PDEs in two or more dimensions. Unlike the traditional CN timestepping scheme, ADI results in solving a set of tridiagonal linear systems at each timestep, the total size of which is the same as the number of unknowns. Since the cost for solving a tridiagonal linear system by standard Gauss elimination (without pivoting) is proportional to the number of unknowns, the cost of each ADI timestep is also proportional to the number of unknowns, therefore, asymptotically optimal. However, in the American option case, the incorporation of the ADI method into the penalty method is not straightforward. Several techniques have been proposed [5], [9] and [8], but more research is needed to make the method as widely used as CN. Furthermore, the studies of convergence and stability of different versions of the ADI timestepping method are a subject for future research as well.

Another possible future work is the application of adaptive mesh methods to the multidimensional Black-Scholes PDE problem. Adaptive mesh methods were used in the numerical solution of the one-dimensional Black-Scholes PDE in [4] and [3]. Also, high-order methods were used in [3], where the emphasis is on pricing one-asset American options. The results in [3] indicate that, despite the discontinuities the solution exhibits, high order of convergence is possible to achieve. Adaptive methods usually compute the optimal placing of the grid points, so that the norm of the error is minimized, and a certain level of accuracy is reached with smaller discretization size, than in non-adaptive methods. However, adaptive mesh methods have not yet been developed and tested for a high-dimensional pricing problem. Therefore, further study on adaptive mesh methods for Exchange options or Spread options is needed.

# Bibliography


[1] S. B, Y. Su, R. Wu, M. C. Fu, and D. Madan, *Pricing American options: A comparison of Monte Carlo simulation approaches*, Journal of Computational Finance, 4 (2001).

[2] F. Black and M. Scholes, *The pricing of options and corporate liabilities*, the Journal of Political Economy, 81 (1973), pp. 637–654.

[3] C. Christara and D. M. Dang, *Adaptive and high-order methods for valuing American options*, J. Comput. Finance, 14 (2011), pp. 73–113.

[4] D. M. Dang, *Adaptive finite difference methods for valuing American options*. M.Sc. Thesis, Department of Computer Science, University of Toronto, Toronto, Ontario, Canada, 132 pgs., 2007.

[5] D. M. Dang, C. C. Christara, and K. R. Jackson, *An efficient graphics processing unit-based parallel algorithm for pricing multi-asset American options*, Concurrency and Computation: Practice and Experience, 24 (2012), pp. 849–866.

[6] P. A. Forsyth and K. R. Vetzal, *Quadratic convergence for valuing American options using a penalty method*, SIAM J. Sci. Comput., 23 (2002), pp. 2095–2122.

[7] P. Glasserman, *Monte Carlo Methods in Financial Engineering*, Springer, 2003.

[8] T. Haentjens and K. J. in 't Hout, *ADI schemes for pricing American options under the Heston model*, Appl. Math. Finance, 22 (2015), pp. 207–237.

[9] V. Heidarpour-Dehkordi and C. C. Christara, *Spread option pricing using ADI methods*, International J. Numerical Analysis and Modelling, (2018). to appear.

[10] J. C. Hull, *Options, Futures, and Other Derivatives*, Pearson, ninth ed., 2014.

[11] I. Karatzas and S. Shreve, *Brownian Motion and Stochastic Calculus*, Graduate Texts in Mathematics, Springer New York, 1991.

[12] E. KIRK, *Correlation in the energy markets*, in Managing Energy Price Risk, V. Kaminski, ed., vol. 1, Risk Publications, 1995, pp. 71–78.

[13] M. LI, S.-J. DENG, AND J. ZHOU, *Closed-form approximations for spread option prices and Greeks*, Journal of Derivatives, 15 (2008), pp. 58–80.

[14] W. MARGRABE, *The value of an option to exchange one asset for another*, J. Finance, 33 (1978), pp. 177–186.

[15] R. C. MERTON, *Option pricing when underlying stock returns are discontinuous*, J. Financial Econ., 3 (1976), pp. 125–144.

[16] R. RANNACHER, *Finite element solution of diffusion problems with irregular data*, Numerische Mathematik, 43 (1984), pp. 309–327.

[17] Y. SAAD, *Iterative Methods for Sparse Linear Systems*, PWS Publishing Company, 1996.

[18] Y. SAAD AND M. H. SCHULTZ, *GMRES: A generalized minimal residual algorithm for solving nonsymmetric linear system*, SIAM J. Sci. Stat. Comput., 7 (1986), pp. 856–869.

[19] E. S. SCHWARTZ, *The valuation of warrants implementing a new approach*, Journal of Financial Economics, 4 (1977), pp. 79–93.

[20] S. SHREVE, *Stochastic Calculus for Finance II: Continuous-Time Models*, vol. 2 of Springer Finance Textbooks, Springer, 2004.

[21] P. WILMOTT, S. HOWISON, AND J. DEWYNNE, *The Mathematics of Financial Derivatives*, Cambridge University Press, 1995.